Oil Production Model
Project, FM1015 Modelling of Dynamic Systems

Bernt Lie

September, 2022

1 Introduction

1.1 General instructions

- This project is a *work requirement* in course FM1015 Modelling of Dynamic Systems:
  - Contributing in the project and the project report is a *work requirement*, and a 50% score is required for the project report to pass this work requirement.
  - Contributing in an oral presentation of the group project is a *work requirement*, and good presentation and understanding of the project report is a requirement to pass the work requirement.
  - The project problem will constitute the *core* of the individual exam December 2[1], 2022.[2]
- You are expected to work in a group of four (± 1); you should establish the groups yourselves. The *group* is expected to write and submit a single group report in a *Canvas Project Group folder*:
  - You are recommended to form groups with a mixture of background (EET, EPE, IIA, PT; different nationalities, etc.) — this will give the group a good variation in process knowledge, programming background, and communication practice.
  - Those who have not established groups by Saturday September 17, 2022, will be placed in groups by me.
  - Do *not* establish a Canvas "Student Group" folder yourself — instead, send an e-mail to the lecturer using the *Canvas Inbox* system, where you state who will be group members, and then the lecturer will establish a *Canvas Project Group folder*.[3]

[1] Tentative date

[2] There may be exam questions unrelated to the project problem. If so, these will constitute a minor part of the exam.

[3] **Reason**: A "Student Group" established by students allows a student to be member in multiple Student Groups, and it is impossible to keep track of whether the student is in a project group or not. The lecturer can establish a type of "Projet Group" where students can only be member of one such Project Group.

  - A mid-way, partial report should be submitted in the Canvas Project Group folder by Friday, October 21, 2022 at 16:00. In this partial report, a dynamic model with first simulation results should be included.
  - A single document final report, PDF format, maximum of 15 pages + a single cover page, is to be submitted in the Canvas group folder by Friday, November 11, 2021 at 23:59.[4]

- The oral project presentation:
  - Each group has 7 minutes *in total* for a presentation (PowerPoint, etc.), and every group member needs to present something. Thus, 1–2 minutes per group member.
  - In preparing the presentation: *remember who the audience is*. The audience is I, the lecturer, who created the group project. Don't waste time by (i) including figures from the task description, (ii) including equations from the task description: I know these figures and equations, and it gets exceedingly boring if I have to listen to 30 repetitions of these figures and equations during the group presentation. Instead, focus on what you have done in the project — remember you have only 7 minutes available to present your work and results.
  - Directly following the presentation will be a brief examination of the work, where every group member will be asked at least one question. In total, 15 minutes will be allotted to each group (presentation + questions).
  - *Campus students* will give the presentation in class on Friday November 18, 2022, starting 10:15 until finish; *industry master students* and on-line students who can be present, are recommended to present in class on this day.
  - *On-line students* and *industry master* students whocan not be present, will give their presentation via MS Teams at a different time — *individual appointments* for Teams presentations will be set up with the lecturer. These presentations should be given *before* November 18, 2022, so as to not delay the publication in Canvas of the lecturer's project solution — which is useful for exam preparation.

The notation used in this project more or less follows the standard notation in the course. This notation may vary from the notation used in the actual problem field.

1.2 Background

Norway is currently (2021) listed as no. 15 on the list of largest petroleum producers in the world, with around 2 million barrels per day (bpd) of production. The largest producer is USA, with ca. 20 million bpd; no. 10 on the list is Kuwait with ca. 3 million bdp. Although Norwegian petroleum production has seen a drop in the period 2000–2020, Fig. 1, petroleum production is still important for the national economy. With fluctuations in the oil price, the current estimate of petroleum production revenues for Norway is ca. US$ 120 billion, which should be compared to Norway's gross domestic product of US$ 350-400 billion.

[4] Yes, maximum 15+1 pages. Not a single page extra for computer code, plots, etc.

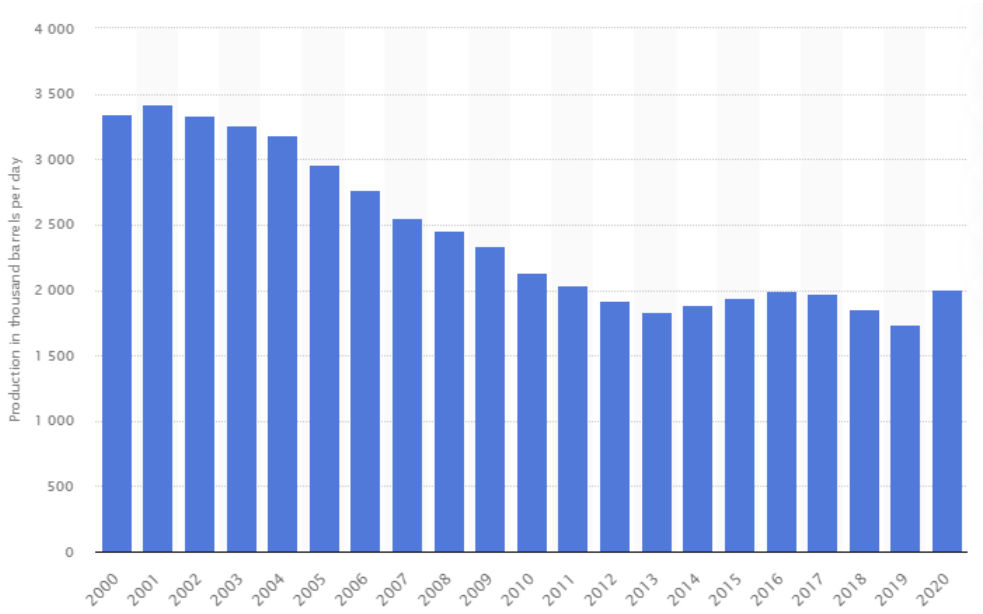

Figure 1: Development in Norwegian oil production. From https://www.statista.com/statistics/265186/oil-production-in-norway-in-barrels-per-day.

Both the COVID-19 pandemic and the current Russian invasion into Ukraine has had considerable impact on oil consumption and oil prices.

Models for the effect of fossil fuel consumption on the environment has given high priority to the transition from fossil fuel to sustainable energy forms. Thus, over a period of some decades, petroleum products will see a dramatic reduction in use as fuel. In the transition period, it is important to reduce the climate footprint of fossil fuel as much as possible. Project "DigiWell" at University of South-Eastern Norway, funded by the Norwegian Research Council and energy company Equinor ASA, aims to reduce this footprint while also reducing uncertainty in the production.

Hydrocarbons are trapped in the subsurface formation of relatively thin slabs of porous rock known as a reservoir. An oil reservoir usually extends up to several hundred kilometers across. In the FM1015 Modelling of Dynamic Systems group project of 2021, the task was to develop a model of an oil reservoir from an aquifer to the heel of the wellbore. The reservoir system is quite slow, with time constants in the order of months. In the project for this year, 2022, the task is to look at oil transport from the heel of the wellbore to the topside separator, which separates the various fluids and residual formation materials. For offshore oil production, the separator is typically located on an oil platform, but it may in principle also be located at the ocean bottom.

In order to understand how oil production is carried out, dynamic models are needed. Such models can also give information about the uncertainty in the model behavior.

1.3 Project aim

This project is designed to give experience in formulating and solving dynamic models of systems, and thus to aid in the learning of the content of course FM1015. Furthermore, the purpose of the project and the presentation is to give the students experience in group work and communication of findings. Finally, because the final exam will be based on the

project work, the project functions as preparation for the final exam.

More specifically, in this group project, oil production models are to be formulated using classical deterministic material and momentum balance principles. The resulting model is to be analyzed briefly wrt. model uncertainty.

A first step in the project is to get familiar with oil production. Not all of this text (Section 2) is required reading!. A *second step* involves formulating and implementing a dynamic model of a single well system from reservoir to manifold, implementing the model, and carrying out some experiments on the model. A *third step* involves formulating a dynamic model of a compressible liquid manifold system. A *fourth step* involves formulating a model of a multiple well system. A *fifth step* involves implementing the multiple well model, and carrying out some experiments on the model. A final step is to write a short report where you focus on your *findings*, and don't repeat text from the task description.

At the end of this project, you will be able to:

1. Uunderstand the basic principles of developing a model of oil production,
2. Solve the oil production model using a computer tool (OpenModelica, Python, Julia, MATLAB, etc.), and
3. Understand how model behavior changes with model uncertainty.

2 Oil Production

2.1 From reservoir to production

2.1.1 Oil field

Figure 2 displays a typical reservoir from the side and the top, with several wellbores: a wellbore is a bore hole from the surface (land, or sea bed) into the formation and through the reservoir to allow reservoir fluid transport to the surface.

An oil field consists of multiple wellbores into the reservoir, and often also multiple reservoirs; the wellbores are then connected through some manifold and the produced fluid is sent from the manifold to some separator. The separator is often placed on land or on some oil platform, but modern systems may also use separators on the sea bed.

2.1.2 Wellbore to separator

For the piping in the wells, Figure 3 displays the geometry of a wellbore, with a production pipe.

The wellbore through the reservoir is often (approximately) horizontal, and may have a length of many km. Reservoir fluids flow into the production pipe through perforations and valves between the heel and toe of the horizontal part. From the heel of the wellbore, the pipe rises more or less vertically through the formation to the formation surface. For some wells, the natural heel pressure is sufficient to transport the production fluid to the manifold. If the heel pressure is insufficient for this transport, two possibilities are: (i) to inject gas to lift the production fluid to the manifold, or (ii) to increase the pressure in the vertical pipe using electric submersible pumps (ESP) so that the production fluid reaches the manifold. In this project, we will consider the case of using an ESP to increase the pressure.

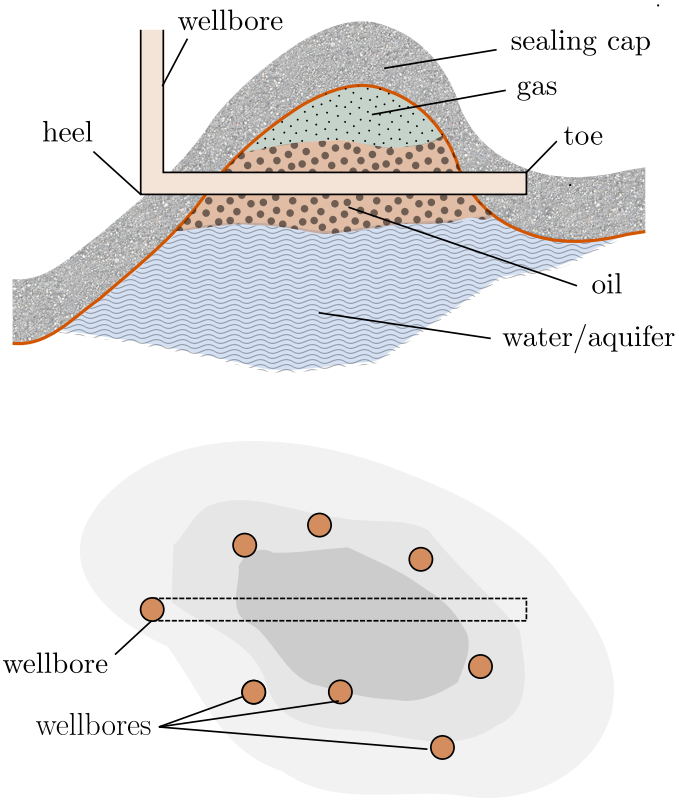

Figure 2: Typical geometry of petroleum reservoir. One reservoir normally contains multiple wellbores.

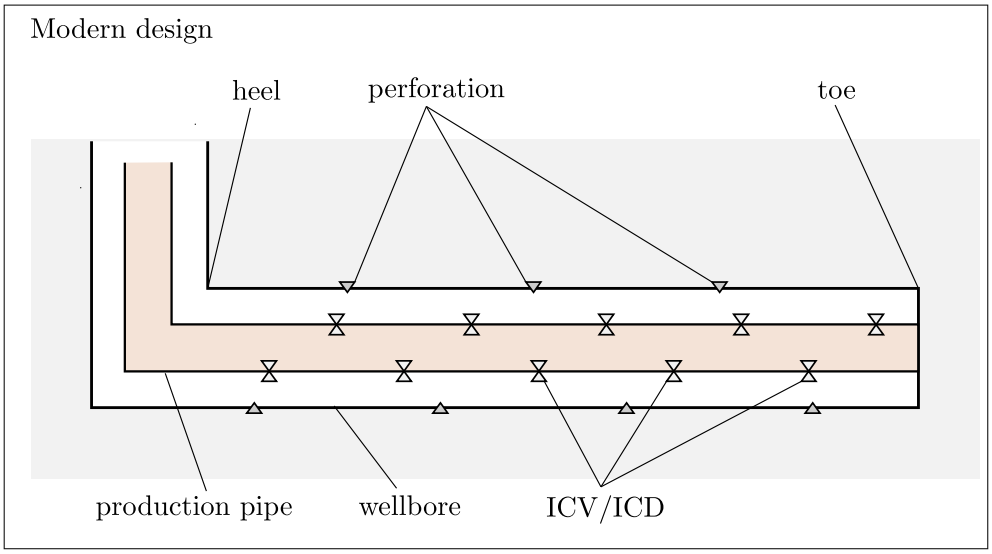

Figure 3: Typical geometry of wellbore, possibly with a production pipe.

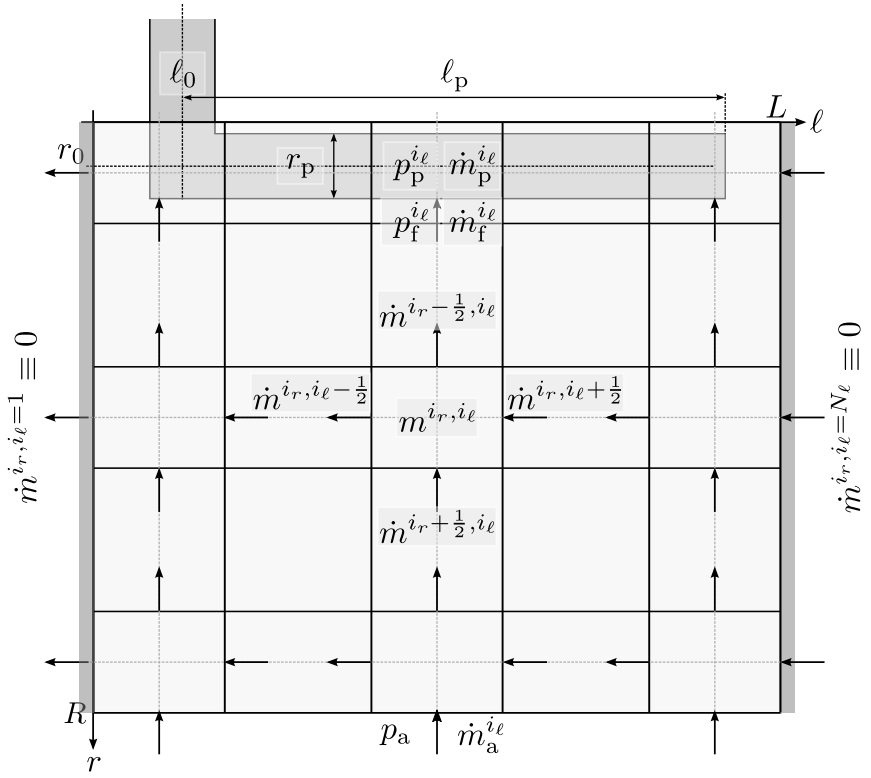

Figure 4: Discretization grid for reservoir. Taken from the project documents for the FM1015 project in 2021.

At the formation surface, multiple wellbores are connected in a manifold. Then the fluids are transported through transport pipes to the separator(s). To aid in the transport, booster pumps are often used to give sufficient pressure for the production fluids to reach the separator. Normally, several parallel transport pipes are needed to give sufficient transport capacity. Water may be pumped into the manifold to increase the water content of the fluid and thereby reduce the viscosity/friction in the transport pipes.

In the separator, the various fluid components (oil, water, gas, etc.) are separated, together with various other components such as formation rock chips, etc.

2.1.3 Reservoir and wellbore

Figure 4 shows the discretization grid for a 2D reservoir with production pipe and aquifer; this was used in the group project of FM1015 Modelling of Dynamic Systems in 2021.

Figure 4 indicates that the reservoir pressure drops from an aquifer pressure p_a (high) within the reservoir, to a pressure p_f (low) in the formation just outside of the wellbore/production pipe. The formation pressure varies along the length of the production pipe, $p_\mathrm{f} = p_\mathrm{f}(\ell)$, and the difference between formation pressure and pressure within the production pipe $p_\mathrm{p}(\ell)$, $\Delta p = p_\mathrm{f}(\ell) - p_\mathrm{p}(\ell)$, constitutes the driving force for transport of reservoir fluid into the production pipe. The production pipe pressure at the heel is denoted p_h, and is given as $p_\mathrm{h} = p_\mathrm{p}(\ell_0)$; see Fig. 4.

2.1.4 Reservoir example

Computation of the relationship between the reservoir and production pipe pressure distribution, and flow of reservoir fluid into the production pipe, is relatively complicated;

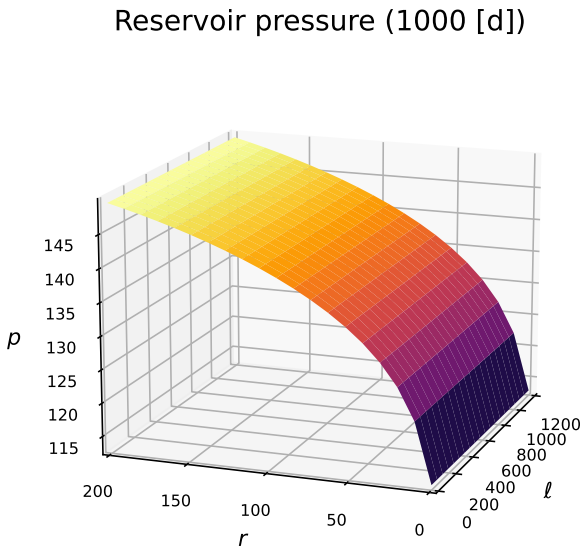

Figure 5: Pressure distribution in reservoir after 1000 days.

this was the topic of the project for course FM1015 Modelling of Dynamic Systems in 2021.

Using semirealistic parameters and operating conditions for the reservoir, Fig. 5 indicates how the pressure varies over the reservoir at day 1000 after production start-up.

Likewise, Fig. 6 shows how pressures near the production pipe vary over time at the heel end.

The main take-away from Section 2.1 is the concept of formation pressure p_{f}, and the observation that changes in the reservoir pressure are quite slow.

2.2 System description

This section presents the system under study in the group project of FM1015 Modelling of Dynamic Systems for 2022.

2.2.1 Single well flowsheet

We will first consider a single oil well as depicted in Fig. 7 in order to get a clear understanding of how things work.

Here, the reservoir formation pressure p_{f} is assumed to be known. The volumetric flow rate out of the wellhead is then given by $\dot{V}_{\mathrm{h}}$ and p_{h}, which are unknowns.

We will, for now, assume constant density in the entire vertical wellbore, and a different density in the transport pipe(s) from the manifold to the separator. In essence, this implies that $\dot{V}_{\mathrm{c}}^{\mathrm{i}} = \dot{V}_{\mathrm{h}}$.

2.2.2 Single transport pipe flowsheet

Here, we consider a single transport pipe from the manifold to the separator, Fig. 8.

Here, the booster pump is assumed to run at constant velocity, and furthermore to yield a constant pressure increase, i.e., $\Delta p_{\mathrm{bp}} = p_{\mathrm{bp}}^{\mathrm{e}} - p_{\mathrm{bp}}^{\mathrm{i}} > 0$ is constant. For simplicity, we will assume a constant density in the transport pipe from the manifold to the separator.

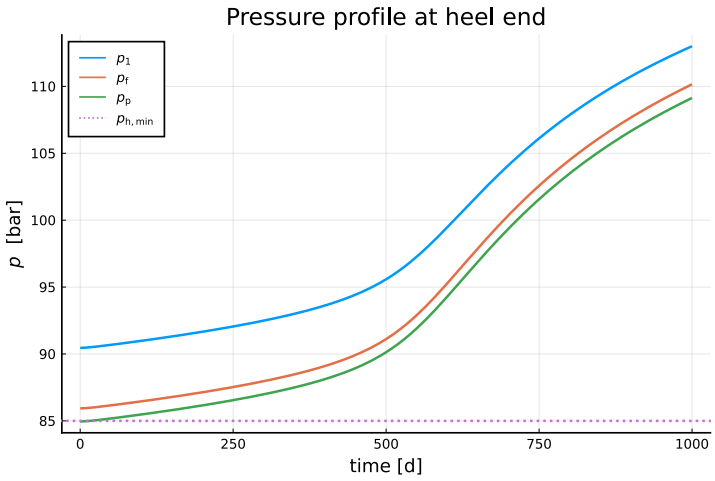

Figure 6: Time evolution of production pipe pressure p_p, pressure p_f just outside of the production pipe (formation interface), and pressure in the first cell p_1 in the reservoir — all *at the heel end* and with constant total production $\dot{V}_h = \dot{V}_w + \dot{V}_o$.

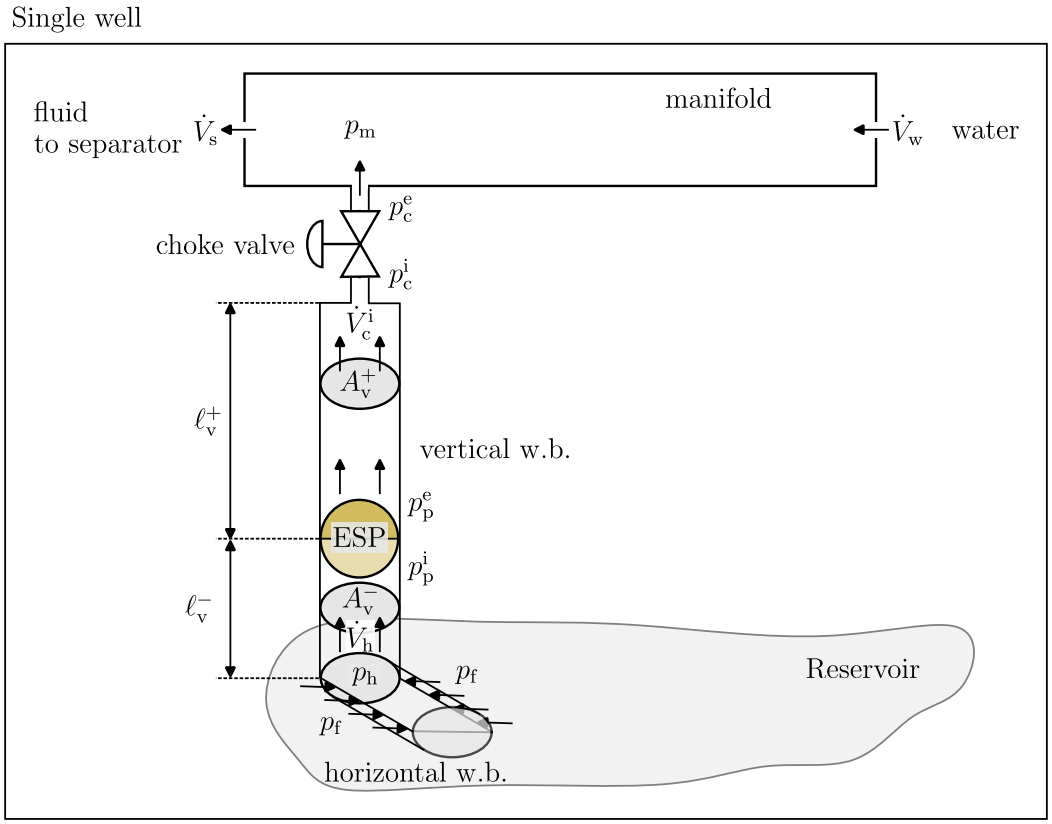

Figure 7: Single well from reservoir via horizontal wellbore, heel of production pipe, vertical wellbore with electric submersible pump (ESP), through choke valve, and into manifold. Water is added to the manifold to reduce the fluid viscosity for further transport towards separator.

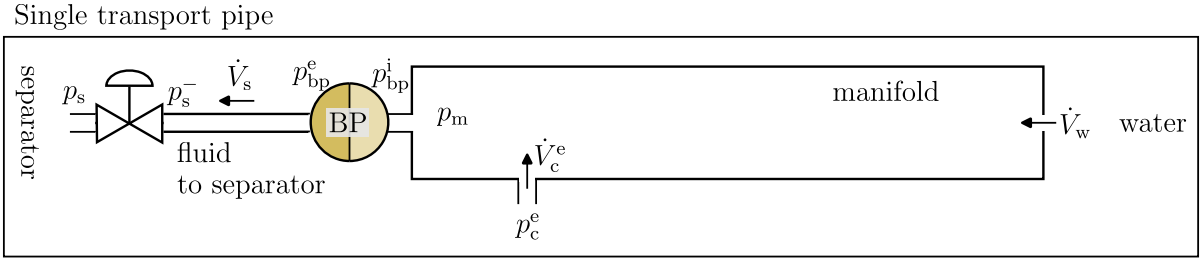

Figure 8: Single transport pipe from manifold, via a constant velocity booster pump to increase the pressure, through the pipe, and ending with the intake valve to the separator. The transport pipe is drawn as a horizontal pipe, but may in principle contain a vertical section up to a floating platform.

2.2.3 Multiple well flowsheet

In reality, the production system merges several boreholes from the same or different reservoirs into the manifold. Furthermore, normally, more than one transport pipe is needed from the manifold to the separator to yield sufficient transport capacity. Figure 9 displays a system with n_w wells and n_t transportation pipes to the separator.

2.3 Property models

2.3.1 Density

For ideal gas, we have $pV = nRT$, which can be rewritten as $pV = \frac{m}{M}RT \Rightarrow pM = \rho RT$, or $\rho = \frac{pM}{RT} = \rho(p, T)$,

$$\rho = \rho(p, T).$$

This expression is one possible formulation of the Equation of State (EoS) for ideal gas, thus the EoS can express how gas density ρ varies with pressure p and temperature T.

In this project, we do not consider a gas, but instead consider a liquid mixture. We seek an EoS for the liquid mixture which relates density with pressure and temperature, $\rho = \rho(p, T)$. The differential of density is

$$\mathrm{d}\rho = \left.\frac{\partial \rho}{\partial p}\right|_T \mathrm{d}p + \left.\frac{\partial \rho}{\partial T}\right|_p \mathrm{d}T. \tag{1}$$

From the discussion of basic thermodynamics in Lie (2022), we can introduce *isothermal compressibility* β_T, and the *coefficient of thermal expansion* α_p.

Figure 10 indicates a typical variation in density of the production liquid with the pressure variation, using data from Appendix A.

2.3.2 Viscosity: simple mixing rules

Linear interpolation In Sharma (2014), a simple linear mixing rule for *kinematic viscosity* ν is used:

$$\nu = \chi_w \nu_w + (1 - \chi_w)\nu_o. \tag{2}$$

With ν known, *dynamic* viscosity μ can be computed (if needed) as

$$\mu = \nu\rho.$$

This linear interpolation model is not physically realistic.

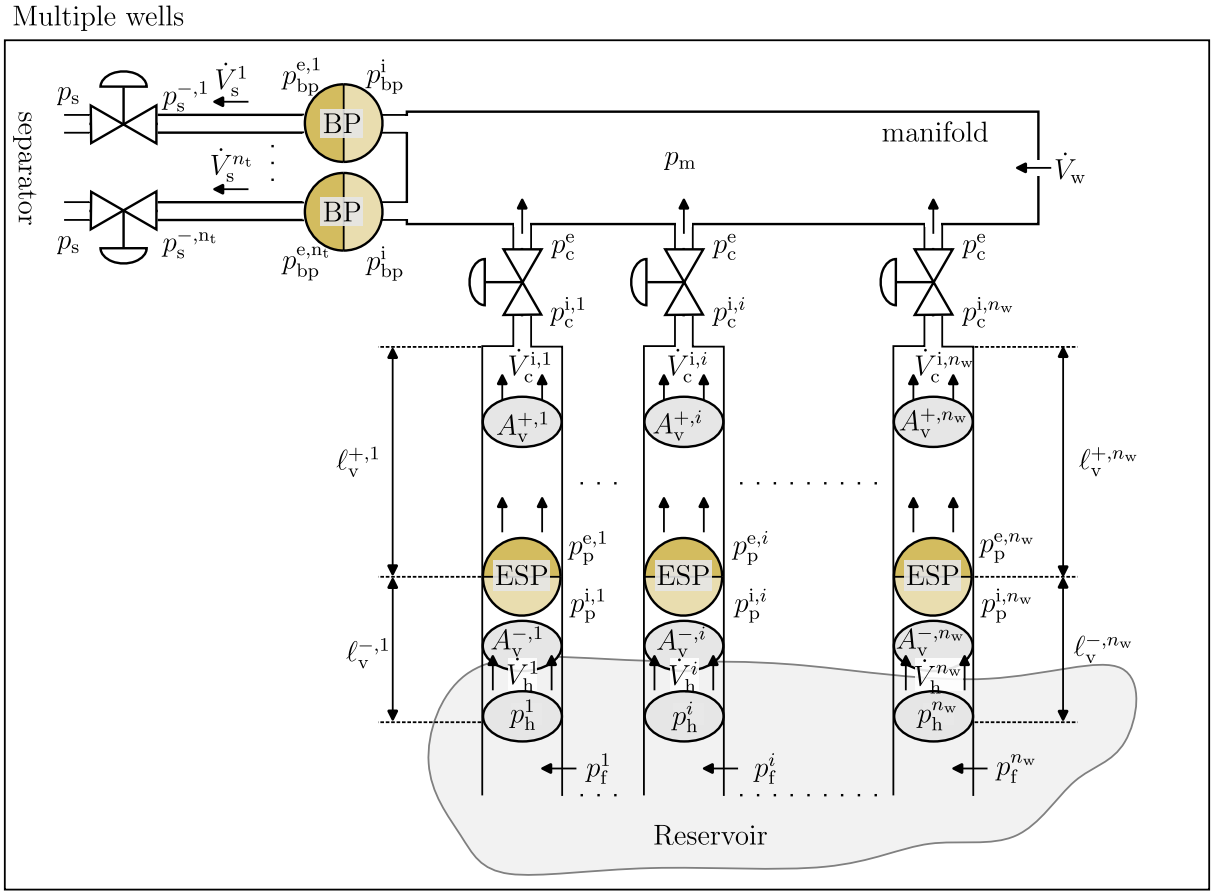

Figure 9: Multiple well system with n_{w} wells similar to the single well in Fig. 7 — possibly coming from different reservoirs, and n_{t} transport pipes to the separator similar to the single pipe in Fig. 8. Observe that for all vertical pipes, $p_{\mathrm{c}}^{\mathrm{e},i} = p_{\mathrm{c}}^{\mathrm{e}} = p_{\mathrm{m}}$ with $i \in \{1, \ldots, n_{\mathrm{w}}\}$, since they all are assumed to be connected to the same manifold pressure. Likewise, for all transport pipes, $p_{\mathrm{s}}^{j} = p_{\mathrm{s}}$ with $j \in \{1, \ldots, n_{\mathrm{t}}\}$ — since we will assume they end up in the same separator.

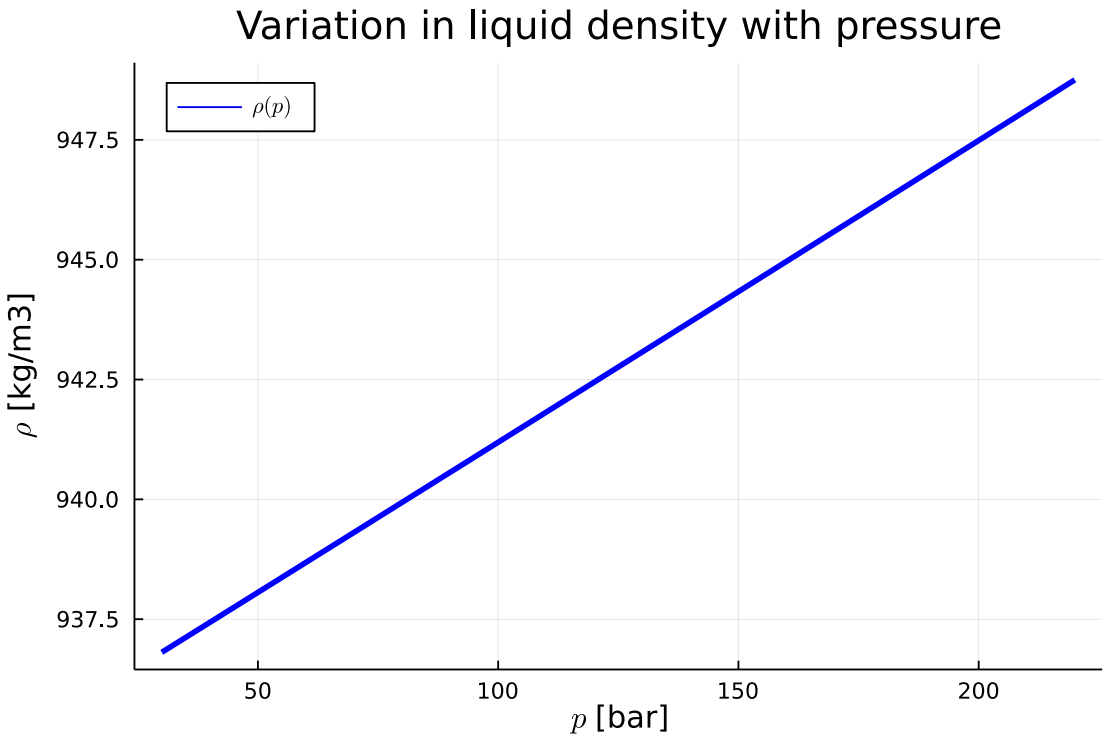

Figure 10: Typical variation in density for production fluid in the pressure range of this project.

Refutas-Chevron model A possible mixing rule for kinematic viscosity, sometimes used in the petroleum industry, the Refutas-Chevron model,[5] introduces the *viscosity blending number* N_ν^j of species j as

$$N_\nu^j = \frac{\ln \nu_j}{\ln\left(10^3 \cdot \nu_j\right)} = \frac{\ln \nu_j}{\ln \nu_j + 3\ln 10}, \tag{3}$$

with mixing rule

$$N_\nu = \chi_\mathrm{w} N_\nu^\mathrm{w} + (1 - \chi_\mathrm{w})\, N_\nu^\mathrm{o}. \tag{4}$$

The kinematic viscosity of the mixture is then found as

$$\nu = 10^{-3N/(N-1)}. \tag{5}$$

In Eqs. 3–5, it is assumed that the kinematic viscosity is given in units cSt.

The above model is highly questionable for oil-water mixtures, because oil and water is immiscible and will form an emulsion, leading to a mixture viscosity that is *higher* than the viscosity of oil for some water cut.

Viscosity model in project In reality, immiscible mixtures may form an emulsion. Section 2.3.3 discusses viscosity for emulsion — included for the interested reader, and *not required reading* for solving the project. Figure 12 shows how the linear model in Eq. 2 and the Refutas-Chevron model in Eqs. 3–5 compare with more realistic models for emulsions.

In this group project, the linear model in Eq. 2 should be used for very simple reasons:

[5] `https://neutrium.net/fluid-flow/estimating-the-viscosity-of-mixtures/`

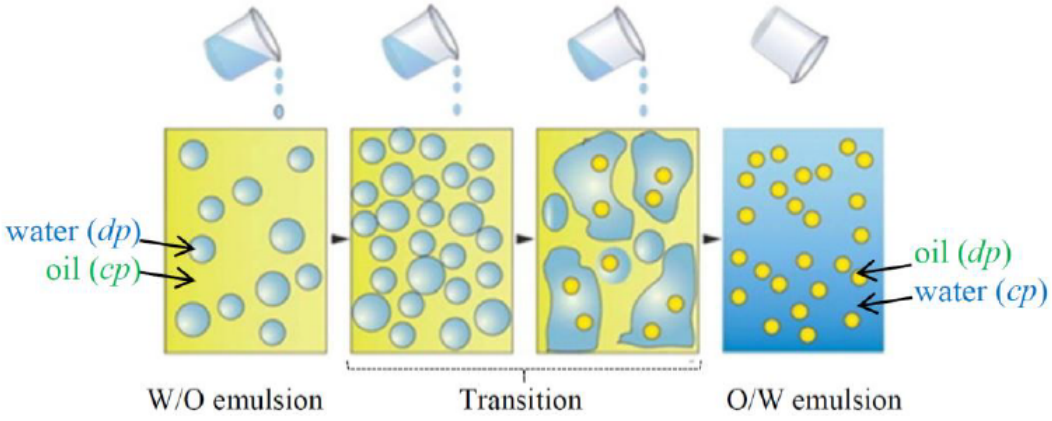

Figure 11: Transition from water-in-oil emulsion towards oil-in-water emulsion. From Justiniano & Romero (2021).

- The equipment dimensions, e.g., pump constants, valve constants provided in appendices, etc., are based on the linear model, and if we change to a more realistic viscosity model, it might be necessary to change the equipment data.
- The linear viscosity model is sufficient for studying the *principles* of modeling.

2.3.3 Viscosity of liquids with emulsion*[6]

Effect of emulsion Water and oil are immiscible fluids and establish an emulsion when mixing. Figure 11 displays how (pure) crude oil gradually is mixed with water as the water content increases, and how this changes the mixture from oil forming the continuous phase ("cp") and water the disperse phase ("dp") (water-in-oil emulsion; W/O emulsion) through a transition towards the case of water forming the continuous phase while oil is the dispersed phase (oil-in-water emulsion; O/W emulsion).

The important aspect of this is that when aggressively agitated, dispersed water in oil (W/O emulsion) increases the viscosity from that of crude oil. The increase is exponential until at a certain *inversion point*, water becomes the continuous phase where the mixture viscosity drops to approximately that of water.

Phase inversion The water fraction (water cut) χ_{w} where the transition from water-in-oil emulsion to oil-in-water emulsion takes place has been studied extensively, Brauner & Ullmann (2002). Based on theoretical models, an inversion model of equal velocity for water and oil between *flat plates* is proposed as

$$\frac{\chi_{\mathrm{o}}^{\mathrm{i}}}{\chi_{\mathrm{w}}^{\mathrm{i}}} = \left(\frac{\mu_{\mathrm{o}}}{\mu_{\mathrm{w}}}\right)^{a} \left(\frac{\rho_{\mathrm{o}}}{\rho_{\mathrm{w}}}\right)^{b} \tag{6}$$

where $\chi_{\mathrm{w}}^{\mathrm{i}} + \chi_{\mathrm{o}}^{\mathrm{i}} = 1$, with $a = 0.5$ and $b = 0$ for laminar flow. Using $\chi_{\mathrm{w}}^{\mathrm{i}} + \chi_{\mathrm{o}}^{\mathrm{i}} = 1$, Eq. 6 can be expressed wrt. $\chi_{\mathrm{w}}^{\mathrm{i}}$ as

$$\chi_{\mathrm{w}}^{\mathrm{i}} = \frac{1}{1 + \left(\frac{\mu_{\mathrm{o}}}{\mu_{\mathrm{w}}}\right)^{a} \left(\frac{\rho_{\mathrm{o}}}{\rho_{\mathrm{w}}}\right)^{b}}. \tag{7}$$

[6]This section is marked * to indicate that it is meant for the interested reader. It is not necessary to read this section to solve the project.

For finding a and b by data regression, taking the logarithm of Eq. 6 leads to a model linear in the parameters,

$$\ln\left(\frac{\chi_{\mathrm{o}}^{\mathrm{i}}}{\chi_{\mathrm{w}}^{\mathrm{i}}}\right) = a\ln\left(\frac{\mu_{\mathrm{o}}}{\mu_{\mathrm{w}}}\right) + b\ln\left(\frac{\rho_{\mathrm{o}}}{\rho_{\mathrm{w}}}\right) \tag{8}$$

For turbulent flow between flat plates, linear regression was found to give $a \approx 0.3$ and $b \approx 1.15$.

For *pipe flow*, Brauner & Ullmann (2002) proposed $a = 0.4$ and $b = 0.6$ based on theoretical considerations. Furthermore by fitting literature data to Eq. 8, they found $a \approx 0.3$ and $b = 0.37$.

Here, with $a = 0.4$ and $b = 0.6$, we observe that

$$\left(\frac{\mu_{\mathrm{o}}}{\mu_{\mathrm{w}}}\right)^{0.4}\left(\frac{\rho_{\mathrm{o}}}{\rho_{\mathrm{w}}}\right)^{0.6} = \left(\frac{\nu_{\mathrm{o}}}{\nu_{\mathrm{w}}}\right)^{0.4}\frac{\rho_{\mathrm{o}}}{\rho_{\mathrm{w}}}$$

where kinematic viscosity ν_j is given by $\nu_j \triangleq \mu_j/\rho_j$. With $a = 0.4$ and $b = 0.6$, Eq. 7 leads to

$$\chi_{\mathrm{w}}^{\mathrm{i}} = \frac{1}{1+\left(\frac{\mu_{\mathrm{o}}}{\mu_{\mathrm{w}}}\right)^{0.4}\left(\frac{\rho_{\mathrm{o}}}{\rho_{\mathrm{w}}}\right)^{0.6}} = \frac{1}{1+\left(\frac{\nu_{\mathrm{o}}}{\nu_{\mathrm{w}}}\right)^{0.4}\frac{\rho_{\mathrm{o}}}{\rho_{\mathrm{w}}}}. \tag{9}$$

The Einstein model Following Bulgarelli et al. (2021), in a first viscosity model for a liquid (continuous phase) with dispersed solids, Einstein developed a model for dilute mixtures with disperse fraction $\chi_{\mathrm{d}} < 0.02$,

$$\frac{\mu}{\mu_{\mathrm{c}}} = 1 + 2.5\chi_{\mathrm{d}}$$

where μ is the dynamic viscosity of the mixture, and μ_{c} the dynamic viscosity of the continuous phase. For liquid-liquid mixtures, it is common to extrapolate and replace the solid dispersed values with liquid dispersed values. In the case of an oil-water mixture, for the W/O emulsion, we have

$$\frac{\mu}{\mu_{\mathrm{o}}} = 1 + 2.5\chi_{\mathrm{w}}$$

while for the O/W emulsion, we have

$$\frac{\mu}{\mu_{\mathrm{w}}} = 1 + 2.5\chi_{\mathrm{o}} = 1 + 2.5\left(1 - \chi_{\mathrm{w}}\right).$$

The Einstein model results in a discontinuous transition from water-in-oil to oil-in-water emulsion, were we could use the Brauner-Ullmann model for $\chi_{\mathrm{w}}^{\mathrm{i}}$, Eq. 7. It follows that the Einstein mixture viscosity is given by

$$\mu = \begin{cases} \mu_{\mathrm{o}}\left(1 + 2.5\chi_{\mathrm{w}}\right), & \chi_{\mathrm{w}} \le \chi_{\mathrm{w}}^{\mathrm{i}} \\ \mu_{\mathrm{w}}\left(3.5 - 2.5\chi_{\mathrm{w}}\right), & \chi_{\mathrm{w}} > \chi_{\mathrm{w}}^{\mathrm{i}}. \end{cases}$$

The Taylor modification of Einstein's model In an extension of Einstein's model for liquid-liquid mixtures, Taylor included the effect of internal circulation and suggested the modified model

$$\frac{\mu}{\mu_{\mathrm{c}}} = 1 + 2.5\frac{\mu_{\mathrm{d}} + 0.4\mu_{\mathrm{c}}}{\mu_{\mathrm{d}} + \mu_{\mathrm{c}}}\chi_{\mathrm{d}}.$$

The W/O emulsion is then described by

$$\frac{\mu}{\mu_{\rm o}} = 1 + 2.5\frac{\mu_{\rm w} + 0.4\mu_{\rm o}}{\mu_{\rm w} + \mu_{\rm o}}\chi_{\rm w}$$

while the O/W emulsion is described by

$$\frac{\mu}{\mu_{\rm w}} = 1 + 2.5\frac{\mu_{\rm o} + 0.4\mu_{\rm w}}{\mu_{\rm o} + \mu_{\rm w}}\left(1 - \chi_{\rm w}\right).$$

Similar to the Einstein model, the Taylor model results in a discontinuous transition from water-in-oil to oil-in-water emulsion: both are linear in $\chi_{\rm d}$. Using the Brauner-Ullmann model for $\chi_{\rm w}^{\rm i}$, Eq. 7, the Taylor mixture viscosity is

$$\mu = \begin{cases} \mu_{\rm o}\left(1 + 2.5\frac{\mu_{\rm w}+0.4\mu_{\rm o}}{\mu_{\rm w}+\mu_{\rm o}}\chi_{\rm w}\right), & \chi_{\rm w} \le \chi_{\rm w}^{\rm i} \\ \mu_{\rm w}\left(1 + 2.5\frac{\mu_{\rm o}+0.4\mu_{\rm w}}{\mu_{\rm o}+\mu_{\rm w}}\left(1-\chi_{\rm w}\right)\right), & \chi_{\rm w} > \chi_{\rm w}^{\rm i}. \end{cases}$$

The Brinkman model Brinkman included the effect of interactions between droplets in a dense emulsion, and proposed the model

$$\frac{\mu}{\mu_{\rm c}} = \frac{1}{\left(1 - \chi_{\rm d}\right)^{2.5}}.$$

The W/O emulsion is then described by

$$\frac{\mu}{\mu_{\rm o}} = \frac{1}{\left(1 - \chi_{\rm w}\right)^{2.5}}$$

while the O/W emulsion is described by

$$\frac{\mu}{\mu_{\rm w}} = \frac{1}{\left(1 - \chi_{\rm o}\right)^{2.5}} = \frac{1}{\chi_{\rm w}^{2.5}}.$$

Here, we can use the Brauner-Ullmann model for the inversion water cut $\chi_{\rm w}^{\rm i}$. This would lead to a slight discontinuity in the mixture emulsion.

Let us instead assume a continuous transition from water-in-oil to oil-in-water emulsion. We then find the Brinkman inversion water cut $\chi_{\rm w}^{\rm i}$ to be

$$\begin{aligned} \mu\left(\chi_{\rm w}^{\rm i}\right) &= \frac{\mu_{\rm o}}{\left(1 - \chi_{\rm w}^{\rm i}\right)^{2.5}} = \frac{\mu_{\rm w}}{\left(\chi_{\rm w}^{\rm i}\right)^{2.5}} \\ &\Downarrow \\ \chi_{\rm w}^{\rm i} &= \frac{1}{1 + \left(\frac{\mu_{\rm o}}{\mu_{\rm w}}\right)^{0.4}}. \end{aligned} \tag{10}$$

It follows that the Brinkman mixture viscosity is

$$\mu = \begin{cases} \frac{\mu_{\rm o}}{\left(1-\chi_{\rm w}\right)^{2.5}}, & \chi_{\rm w} \le \chi_{\rm w}^{\rm i} \\ \frac{\mu_{\rm w}}{\chi_{\rm w}^{2.5}}, & \chi_{\rm w} > \chi_{\rm w}^{\rm i}. \end{cases}$$

Modified Brinkman model with Taylor exponent In Justiniano & Romero (2021), the Brinkman model is used, but factor 2.5 is replaced by the modified factor according to Taylor's model, i.e.,

$$\frac{\mu}{\mu_{\mathrm{c}}} = \frac{1}{(1-\chi_{\mathrm{d}})^{n_{\mathrm{c}}}}$$

where

$$n_{\mathrm{c}} = 2.5\frac{\mu_{\mathrm{d}} + 0.4\mu_{\mathrm{c}}}{\mu_{\mathrm{d}} + \mu_{\mathrm{c}}}.$$

Here, we can use the Brauner-Ullmann description of the water cut inversion point $\chi_{\mathrm{w}}^{\mathrm{i}}$. Thus, the emulsion dynamic viscosity μ is then given as

$$\mu = \begin{cases} \frac{\mu_{\mathrm{o}}}{(1-\chi_{\mathrm{w}})^{n_{\mathrm{o}}}}, & \chi_{\mathrm{w}} \leq \chi_{\mathrm{w}}^{\mathrm{i}} \\ \frac{\mu_{\mathrm{w}}}{\chi_{\mathrm{w}}^{n_{\mathrm{w}}}}, & \chi_{\mathrm{w}} > \chi_{\mathrm{w}}^{\mathrm{i}} \end{cases}$$

where

$$n_{\mathrm{o}} = 2.5\frac{\mu_{\mathrm{w}} + 0.4\mu_{\mathrm{o}}}{\mu_{\mathrm{w}} + \mu_{\mathrm{o}}}$$
$$n_{\mathrm{w}} = 2.5\frac{\mu_{\mathrm{o}} + 0.4\mu_{\mathrm{w}}}{\mu_{\mathrm{o}} + \mu_{\mathrm{w}}}.$$

Again, the above combination of the Brauner-Ullmann inversion point and the Brinkman model with Taylor exponent leads to a *discontinuous* transition from W/O to O/W emulsion. It is possible to enforce a continuous transition by dropping the Brauner-Ullmann inversion point and procede as with the continuous Brinkman formulation. This will, however, give an implicit expression for $\chi_{\mathrm{w}}^{\mathrm{i}}$:

$$\begin{aligned} \mu\left(\chi_{\mathrm{w}}^{\mathrm{i}}\right) &= \frac{\mu_{\mathrm{o}}}{\left(1-\chi_{\mathrm{w}}^{\mathrm{i}}\right)^{n_{\mathrm{o}}}} = \frac{\mu_{\mathrm{w}}}{\left(\chi_{\mathrm{w}}^{\mathrm{i}}\right)^{n_{\mathrm{w}}}} \\ &\Downarrow \\ 0 &= \mu_{\mathrm{o}}\left(\chi_{\mathrm{w}}^{\mathrm{i}}\right)^{n_{\mathrm{w}}} - \mu_{\mathrm{w}}\left(1-\chi_{\mathrm{w}}^{\mathrm{i}}\right)^{n_{\mathrm{o}}} \end{aligned}$$

where the value from the Brauner-Ullmann inversion point probably is a good initial guess.

Proposal: Brauner-Ullmann continuous model The following viscosity model can be postulated based on the Brauner-Ullmann inversion point, Eq. 11:

$$\frac{\mu}{\mu_{\mathrm{c}}} = \frac{1}{(1-\chi_{\mathrm{d}})^{\alpha}\left(\frac{\rho_{\mathrm{d}}}{\rho_{\mathrm{c}}}\right)^{\beta\cdot\left(\chi_{\mathrm{d}}/\chi_{\mathrm{d}}^{\mathrm{i}}\right)^{\gamma_{\mathrm{c}}}}}. \tag{11}$$

Here, $\chi_{\mathrm{d}}/\chi_{\mathrm{d}}^{\mathrm{i}} = 0$ when $\chi_{\mathrm{d}} = 0$ giving correct viscosities for the pure components, and $\chi_{\mathrm{d}}/\chi_{\mathrm{d}}^{\mathrm{i}} = 1$ at the inversion point. An even more general formulation would replace $\left(\chi_{\mathrm{d}}/\chi_{\mathrm{d}}^{\mathrm{i}}\right)^{\gamma_{\mathrm{c}}}$ with some more general function $f\left(\chi_{\mathrm{d}}\right)$ satisfying $f\left(0\right) = 0$ and $f\left(\chi_{\mathrm{d}}^{\mathrm{i}}\right) = 1$, but there may not be much to gain from this.

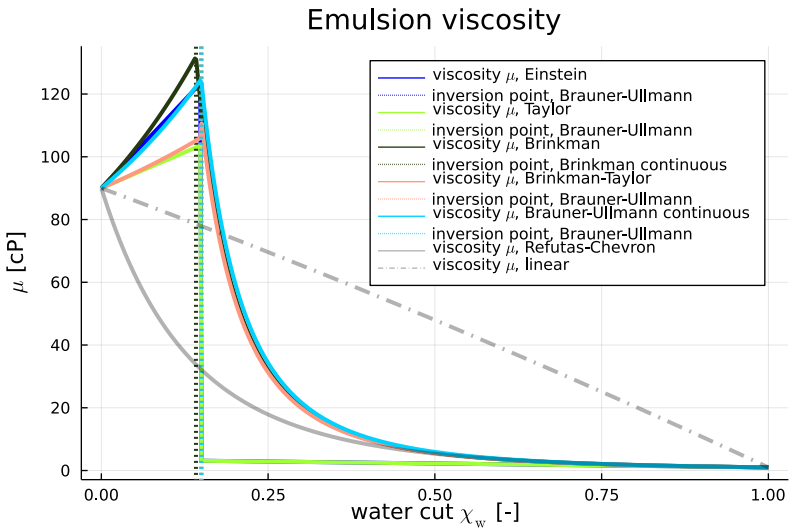

Figure 12: Emulsion viscosity as a function of water cut χ_{w}.

If we want to have a continuous transition from water-in-oil to oil-in-water emulsion, the inversion point $\chi_{\mathrm{w}}^{\mathrm{i}}$ must satisfy

$$
\begin{aligned}
\mu\left(\chi_{\mathrm{w}}^{\mathrm{i}}\right) &= \frac{\mu_{\mathrm{o}}}{(1-\chi_{\mathrm{w}}^{\mathrm{i}})^{\alpha}\left(\frac{\rho_{\mathrm{w}}}{\rho_{\mathrm{o}}}\right)^{\beta\cdot 1^{\gamma_{\mathrm{o}}}}} = \frac{\mu_{\mathrm{w}}}{(\chi_{\mathrm{w}}^{\mathrm{i}})^{\alpha}\left(\frac{\rho_{\mathrm{o}}}{\rho_{\mathrm{w}}}\right)^{\beta\cdot 1^{\gamma_{\mathrm{w}}}}} \\
&\Downarrow \\
\left(\frac{1-\chi_{\mathrm{w}}^{\mathrm{i}}}{\chi_{\mathrm{w}}^{\mathrm{i}}}\right)^{\alpha} &= \frac{\mu_{\mathrm{o}}}{\mu_{\mathrm{w}}}\frac{\left(\frac{\rho_{\mathrm{o}}}{\rho_{\mathrm{w}}}\right)^{\beta}}{\left(\frac{\rho_{\mathrm{w}}}{\rho_{\mathrm{o}}}\right)^{\beta}} = \frac{\mu_{\mathrm{o}}}{\mu_{\mathrm{w}}}\left(\frac{\rho_{\mathrm{o}}}{\rho_{\mathrm{w}}}\right)^{2\beta} \\
&\Downarrow \\
\frac{1-\chi_{\mathrm{w}}^{\mathrm{i}}}{\chi_{\mathrm{w}}^{\mathrm{i}}} &= \left(\frac{\mu_{\mathrm{o}}}{\mu_{\mathrm{w}}}\right)^{1/\alpha}\left(\frac{\rho_{\mathrm{o}}}{\rho_{\mathrm{w}}}\right)^{2\beta/\alpha} \\
&\Downarrow \\
\chi_{\mathrm{w}}^{\mathrm{i}} &= \frac{1}{1+\left(\frac{\mu_{\mathrm{o}}}{\mu_{\mathrm{w}}}\right)^{1/\alpha}\left(\frac{\rho_{\mathrm{o}}}{\rho_{\mathrm{w}}}\right)^{2\beta/\alpha}}.
\end{aligned}
\tag{12}
$$

With $a = 1/\alpha$ and $b = 2\beta/\alpha$, this is the generalized Brauner-Ullmann inversion point as in Eq. 7. Specifically, with $a = 0.4$, $\alpha = 2.5$, and with $b = 0.6$, $\beta = 0.3 \cdot 2.5 = 0.75$. The inversion point is independent of exponent γ_{c}.

Comparison of viscosity models Figure 12 illustrates how the viscosity of the emulsion varies with water cut χ_{w} for the models described in the prequel.

Observe specifically that the inversion point found from the Brauner-Ullmann equation, Eq. 9, is very close to the one found assuming continuity in the Brinkman model, Eq. 10.

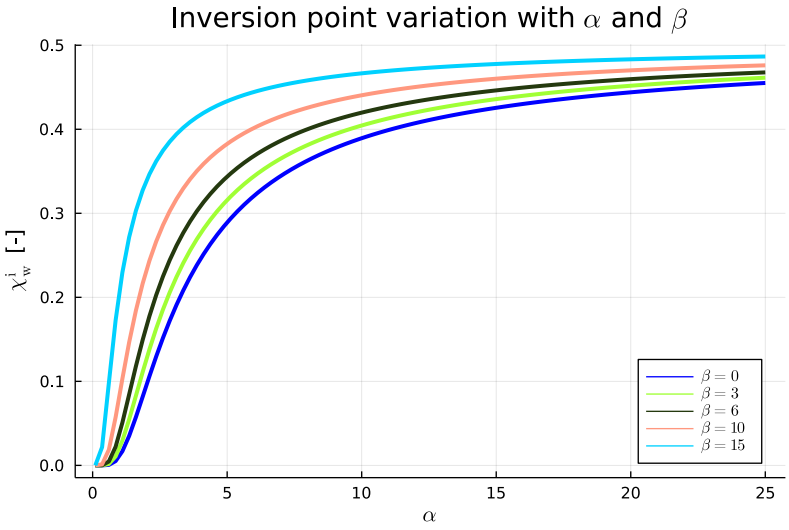

Figure 13: Variation in inversion point $\chi_{\mathrm{w}}^{\mathrm{i}}$ with parameters α and β.

Industry practice models In practice, an experimental approach is often used. One possible approach is to use the postulated Brauner-Ullmann model of Eq. 11,

$$\frac{\mu}{\mu_{\mathrm{c}}} = \frac{1}{(1-\chi_{\mathrm{d}})^{\alpha}\left(\frac{\rho_{\mathrm{d}}}{\rho_{\mathrm{c}}}\right)^{\beta\cdot\left(\chi_{\mathrm{d}}/\chi_{\mathrm{d}}^{\mathrm{i}}\right)^{\gamma_{\mathrm{c}}}}},$$

which is an extension of the Brinkman model. Based on a measured friction pressure drop Δp_{f} for a number of water cuts χ_{w}, it is necessary to describe how the pressure drop relates to the mixture viscosity, typically using some Darcy-Weisbach expression or related expressions. Next, the model parameters (here: α, β, γ_{o}, γ_{w}) are tuned to fit the experimental data.

It is of interest to see how the location of the inversion point varies with α and β in the Brauner-Ullmann model of Eq. 12,

$$\chi_{\mathrm{w}}^{\mathrm{i}} = \frac{1}{1+\left(\frac{\mu_{\mathrm{o}}}{\mu_{\mathrm{w}}}\right)^{1/\alpha}\left(\frac{\rho_{\mathrm{o}}}{\rho_{\mathrm{w}}}\right)^{2\beta/\alpha}}.$$

Figure 13 indicates how χ_{w} varies with $\alpha \in [0.1, 25]$ for $\beta \in \{0, 3, 6, 10, 15\}$.

As Fig. 13 indicates, the inversion point lies in the range $\chi_{\mathrm{w}}^{\mathrm{i}} \in [0, 0.5]$ for values of (α, β).

It is also of interest to see how the choice of parameters α, β, and γ_{d} influence viscosity $\mu(\chi_{\mathrm{w}})$ of the proposed Brauner-Ullmann continuous model in Eq. 11. First, we consider parameters α, β, Fig. 14, and next we consider parameter γ_{c}; Fig. 15.

Fitting model to data Suppose we have experimental data and measure the location of the inversion point $\chi_{\mathrm{w}}^{\mathrm{i}}$, as well as the mixture viscosity just left of the inversion point, $\lim_{\chi_{\mathrm{w}} \to \chi_{\mathrm{w}}^{\mathrm{i},-}} \mu(\chi_{\mathrm{w}})$. Then we trivially know the points

$$\frac{\chi_{\mathrm{o}}^{\mathrm{i}}}{\chi_{\mathrm{w}}^{\mathrm{i}}} = \frac{1-\chi_{\mathrm{w}}^{\mathrm{i}}}{\chi_{\mathrm{w}}^{\mathrm{w}}}$$

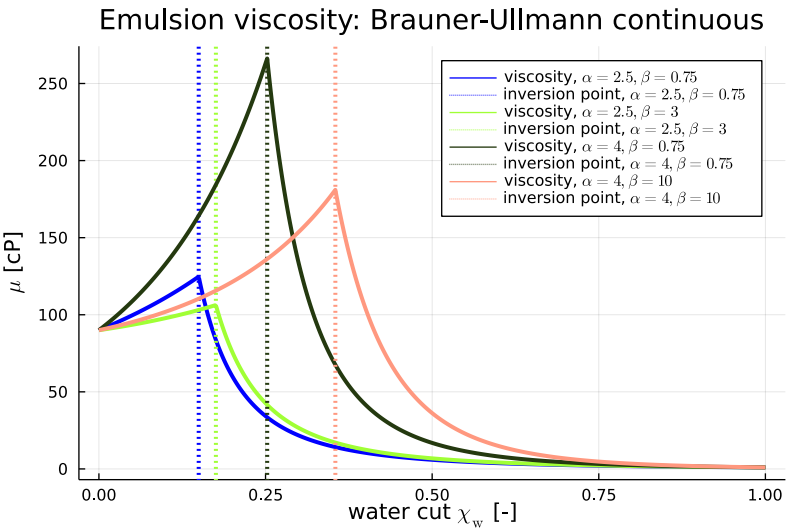

Figure 14: Variation in viscosity $\mu(\chi_w)$ with parameters α and β.

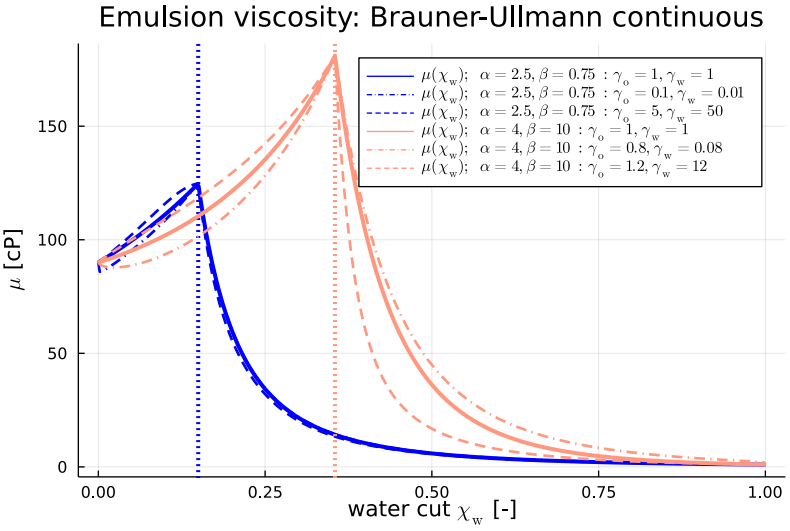

Figure 15: Variation in viscosity $\mu(\chi_w)$ with parameter γ_c.

and,

$$\lim_{\chi_{\mathrm{w}} \to \chi_{\mathrm{w}}^{\mathrm{i},-}} \frac{\mu\left(\chi_{\mathrm{w}}\right)}{\mu_{\hat{\mathrm{o}}}\left(\chi_{\mathrm{w}}\right)}.$$

The proposed Brauner-Ullmann continuous viscosity model in Eq. 11,

$$\frac{\mu}{\mu_{\mathrm{c}}} = \frac{1}{\left(1-\chi_{\mathrm{d}}\right)^{\alpha}\left(\frac{\rho_{\mathrm{d}}}{\rho_{\mathrm{c}}}\right)^{\beta\cdot\left(\chi_{\mathrm{d}}/\chi_{\mathrm{d}}^{\mathrm{i}}\right)^{\gamma_{\mathrm{c}}}}},$$

gives us 4 parameters for tuning: α, β, γ_{o}, and γ_{w}.

With Eq. 6, we have

$$\begin{gathered}\frac{\chi_{\mathrm{o}}^{\mathrm{i}}}{\chi_{\mathrm{w}}^{\mathrm{i}}} = \left(\frac{\mu_{\mathrm{o}}}{\mu_{\mathrm{w}}}\right)^{a}\left(\frac{\rho_{\mathrm{o}}}{\rho_{\mathrm{w}}}\right)^{b} \\ \Downarrow \\ \ln\left(\frac{\chi_{\mathrm{o}}^{\mathrm{i}}}{\chi_{\mathrm{w}}^{\mathrm{i}}}\right) = a\ln\left(\frac{\mu_{\mathrm{o}}}{\mu_{\mathrm{w}}}\right) + b\ln\left(\frac{\rho_{\mathrm{o}}}{\rho_{\mathrm{w}}}\right).\end{gathered}$$

Inserting the relationship between (a, b) and (α, β), we find

$$\ln\left(\frac{\chi_{\mathrm{o}}^{\mathrm{i}}}{\chi_{\mathrm{w}}^{\mathrm{i}}}\right) = \frac{1}{\alpha}\ln\left(\frac{\mu_{\mathrm{o}}}{\mu_{\mathrm{w}}}\right) + \frac{2\beta}{\alpha}\ln\left(\frac{\rho_{\mathrm{o}}}{\rho_{\mathrm{w}}}\right)$$

which can be re-arranged into

$$\ln\left(\frac{\mu_{\mathrm{o}}}{\mu_{\mathrm{w}}}\right) = \alpha\ln\left(\frac{\chi_{\mathrm{o}}^{\mathrm{i}}}{\chi_{\mathrm{w}}^{\mathrm{i}}}\right) - \beta\ln\left(\frac{\rho_{\mathrm{o}}}{\rho_{\mathrm{w}}}\right)^{2}. \tag{13}$$

With Eq. 11, we have

$$\begin{gathered}\frac{\mu^{\mathrm{i}}}{\mu_{\mathrm{o}}} = \lim_{\chi_{\mathrm{w}} \to \chi_{\mathrm{w}}^{\mathrm{i},-}} \frac{\mu\left(\chi_{\mathrm{w}}\right)}{\mu_{\mathrm{o}}\left(\chi_{\mathrm{w}}\right)} = \frac{1}{\left(1-\chi_{\mathrm{w}}^{\mathrm{i}}\right)^{\alpha}\left(\frac{\rho_{\mathrm{w}}}{\rho_{\mathrm{o}}}\right)^{\beta\cdot 1}} = \frac{\left(\frac{\rho_{\mathrm{o}}}{\rho_{\mathrm{w}}}\right)^{\beta}}{\left(1-\chi_{\mathrm{w}}^{\mathrm{i}}\right)^{\alpha}} \\ \Downarrow \\ \ln\left(\frac{\mu^{\mathrm{i}}}{\mu_{\mathrm{o}}}\right) = \beta\ln\left(\frac{\rho_{\mathrm{o}}}{\rho_{\mathrm{w}}}\right) - \alpha\ln\left(1-\chi_{\mathrm{w}}^{\mathrm{i}}\right).\end{gathered} \tag{14}$$

It follows that we have two equations in the two unknowns (α, β), 13 and 14:

$$\begin{aligned}\alpha\ln\left(\frac{\chi_{\mathrm{o}}^{\mathrm{i}}}{\chi_{\mathrm{w}}^{\mathrm{i}}}\right) - \beta\ln\left(\frac{\rho_{\mathrm{o}}}{\rho_{\mathrm{w}}}\right)^{2} &= \ln\left(\frac{\mu_{\mathrm{o}}}{\mu_{\mathrm{w}}}\right) \\ -\alpha\ln\left(1-\chi_{\mathrm{w}}^{\mathrm{i}}\right) + \beta\ln\left(\frac{\rho_{\mathrm{o}}}{\rho_{\mathrm{w}}}\right) &= \ln\left(\frac{\mu^{\mathrm{i}}}{\mu_{\mathrm{o}}}\right)\end{aligned}$$

which can conveniently be posed as a matrix equation

$$\begin{pmatrix} \ln\left(\frac{\chi_{\mathrm{o}}^{\mathrm{i}}}{\chi_{\mathrm{w}}^{\mathrm{i}}}\right) & -\ln\left(\frac{\rho_{\mathrm{o}}}{\rho_{\mathrm{w}}}\right)^{2} \\ -\ln\left(1-\chi_{\mathrm{w}}^{\mathrm{i}}\right) & \ln\left(\frac{\rho_{\mathrm{o}}}{\rho_{\mathrm{w}}}\right) \end{pmatrix} \begin{pmatrix} \alpha \\ \beta \end{pmatrix} = \begin{pmatrix} \ln\left(\frac{\mu_{\mathrm{o}}}{\mu_{\mathrm{w}}}\right) \\ \ln\left(\frac{\mu^{\mathrm{i}}}{\mu_{\mathrm{o}}}\right) \end{pmatrix} \tag{15}$$

and solved to yield (α, β).

Finally, for the proposed Brauner-Ullmann viscosity expression, we can tune γ_{o} and γ_{w} to find a best possible shape of the viscosity model.

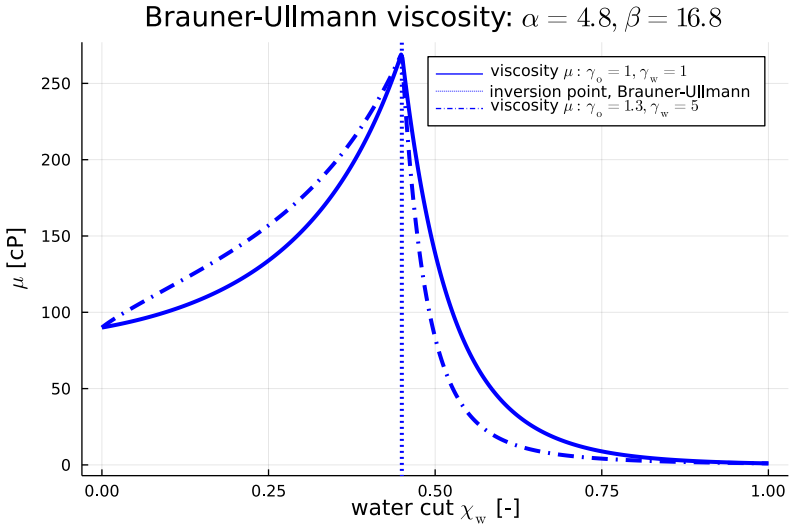

Figure 16: Variation in viscosity $\mu(\chi_w)$ assuming $\chi_w^i = 0.45$ and $\mu^i/\mu_o = 3$; $\gamma_o = \gamma_w = 1$ as well as $\gamma_o = 1.3$, $\gamma_w = 5$.

Example. Tuning proposed continuous Brauner-Ullmann model

Let us assume that $\chi_w^i = 0.45$, $\mu^i/\mu_o = 3.0$, while ρ_j and ν_j are as given in Table 1 and $\mu_j = \rho_j \nu_j$. Using Eq. 15, we find

$$\begin{pmatrix} \ln\left(\frac{1-0.45}{0.45}\right) & -\ln\left(\frac{900}{1000}\right)^2 \\ -\ln(1-0.45) & \ln\left(\frac{900}{1000}\right) \end{pmatrix} \begin{pmatrix} \alpha \\ \beta \end{pmatrix} = \begin{pmatrix} \ln\left(\frac{900 \cdot 100 \cdot 10^{-6}}{1000 \cdot 1 \cdot 10^{-6}}\right) \\ \ln(3) \end{pmatrix}$$

$$\Downarrow$$

$$\begin{pmatrix} \alpha \\ \beta \end{pmatrix} \approx \begin{pmatrix} 4.8 \\ 16.8 \end{pmatrix}.$$

The resulting viscosity of the mixture is shown in Fig. 16 with $\gamma_o = \gamma_w = 1$ and with $\gamma_o = 1.3$ and $\gamma_w = 5$ in the proposed Brauner-Ullmann model with inversion point continuity.

2.4 Equipment models

2.4.1 Reservoir production via Productivity Index

In this course project of course FM1015 Modelling of Dynamic Systems for 2022, the focus is on the flow of reservoir fluids/production fluids from the production pipe *heel* to the topside separator. The dynamics of this part of oil production is much faster than the dynamics of the reservoir as indicated in Fig. 6. Instead of using a complicated reservoir model, we will use a simplified model of the relationship between total production $\dot{V}_h$ at the wellbore heel, the reservoir pressure, and the pressure p_h at the heel.

Specifically, we will write the total production as

$$\dot{V}_h = C_{\dot{V}}^{pi} \frac{p_f - p_h}{p_{pi}^{\varsigma}} \tag{16}$$

where $C_{\dot{V}}^{pi}$ is the *Productivity Index constant*, i.e., a scaled *Productivity Index*,[7] p_f is the formation pressure just outside of the wellbore at some specified position, p_h is the wellbore

[7]The productivity index $\mathfrak{I}_p$ is commonly given as $\mathfrak{I}_p = \dot{V}_{pi}/p^{\varsigma}$.

heel pressure, and $p_{\mathrm{pi}}^{\varsigma}$ is a scaling pressure with the same units as p_{f} and p_{h}. The advantage with the production expression in Eq. 16 is that unit conversion is simple since $\frac{p_{\mathrm{f}}-p_{\mathrm{h}}}{p_{\mathrm{pi}}^{\varsigma}}$ is dimensionless, hence $C_{\dot{V}}^{\mathrm{pi}}$ has the same unit as $\dot{V}_{\mathrm{h}}$.

The alternative to the simple description in Eq. 16 is a more realistic, complicated reservoir model as in the FM1015 project of 2021.

2.4.2 Pump models

Generic pump Typically, pump models are given as

$$\Delta p_{\mathrm{p}} = \rho g h_{\mathrm{p}} \tag{17}$$

where the pump *head* $h_{\mathrm{p}} = h_{\mathrm{p}}\left(\dot{V}, f_{\mathrm{p}}\right)$ with f_{p} the control input — the rotational frequency of the pump in Hz. Some pumps are operated without changing the rotational frequency of the pump; in that case, the head will only depend on the volumetric flow rate $\dot{V}$.

Electric Submersible Pump Sharma (2014) gives the head h_{p} of a multi-stage electric submersible pump (ESP). Here, we have *rewritten* Sharma's model in dimensionless form

$$\frac{h_{\mathrm{p}}\left(\dot{V}, f_{\mathrm{p}}\right)}{h_{\mathrm{p}}^{\varsigma}} = \left(\frac{f_{\mathrm{p}}}{f_{\mathrm{p},0}}\right)^2 + a_1 \frac{f_{\mathrm{p}}}{f_{\mathrm{p},0}} \frac{\dot{V}}{\dot{V}^{\varsigma}} + a_2 \left(\frac{\dot{V}}{\dot{V}^{\varsigma}}\right)^2 + a_3 \frac{f_{\mathrm{p},0}}{f_{\mathrm{p}}} \left(\frac{\dot{V}}{\dot{V}^{\varsigma}}\right)^3. \tag{18}$$

In Eq. 18, $h_{\mathrm{p}}^{\varsigma}$ is a scaling head, f_{p} is the pump rotational frequency in the same unit as that of the nominal rotational frequency $f_{\mathrm{p},0}$, $\dot{V}$ is the actual volumetric flow rate out of the pump, $\dot{V}^{\varsigma}$ a scaling flow rate, and $a_1, \ldots, a_3$ are dimensionless model parameters[8]. This formulation makes it simple to change units of h_{p}, f_{p}, and $\dot{V}$.

Booster pump Booster pumps are needed to transport the production fluid from the manifold to the separator. Sharma (2014) suggests that for these booster pumps, the pressure head h_{bp} is independent of the volumetric flow rate; essentially, the expression for the head just contains the first term on the right hand side of Eq. 18,

$$\frac{h_{\mathrm{bp}}\left(f_{\mathrm{p}}\right)}{h_{\mathrm{bp}}^{\varsigma}} = \left(\frac{f_{\mathrm{bp}}}{f_{\mathrm{bp},0}}\right)^2 = \frac{\rho g h_{\mathrm{bp}}}{\rho g h_{\mathrm{bp}}^{\varsigma}} = \frac{\Delta p_{\mathrm{bp}}\left(f_{\mathrm{p}}\right)}{\Delta p_{\mathrm{bp}}^{\varsigma}} \tag{19}$$

Here, $\Delta p_{\mathrm{bp}}\left(f_{\mathrm{bp}}\right)$ is the pressure increase at the given pump frequency/speed f_{bp}, in the same unit as $\Delta p_{\mathrm{bp}}^{\varsigma}$ — which is the pressure increase at the nominal pump frequency $f_{\mathrm{bp},0}$.

[8]Here, a_j is dimensionless, while in Sharma (2014) his parameters a_j have dimensions. This implies that the values of a_j here are different from those of a_j in Sharma (2014).

2.4.3 Valve

Basis: Bernoulli's equation Bernoulli's law for horizontal flow, Lie (2022), combined with steady mass balance $\dot{m}_\mathrm{i} = \dot{m}_\mathrm{e} = \dot{m}$ for a valve, and $\dot{m} = \rho_\mathrm{i}\dot{V}_\mathrm{i} = \rho_\mathrm{e}\dot{V}_\mathrm{e}$, leads to

$$p_\mathrm{i}\dot{V}_\mathrm{i} + \frac{1}{2}\dot{m}_\mathrm{i}v_\mathrm{i}^2 = p_\mathrm{e}\dot{V}_\mathrm{e} + \frac{1}{2}\dot{m}_\mathrm{e}v_\mathrm{e}^2$$
$$\Downarrow$$
$$\dot{m} = \sqrt{2\frac{\frac{p_\mathrm{i}}{\rho_\mathrm{i}} - \frac{p_\mathrm{e}}{\rho_\mathrm{e}}}{\frac{1}{(\rho_\mathrm{e}A_\mathrm{e})^2} - \frac{1}{(\rho_\mathrm{i}A_\mathrm{i})^2}}}.$$

In Lie (2022), a simplified version of this expression is given where it is assumed that $\rho_\mathrm{i} = \rho_\mathrm{e} = \rho$. Here, we will consider the possibility that $\rho_\mathrm{i} \neq \rho_\mathrm{e}$. This expression for mass flow rate indicates that $\dot{m}$ depends on the pressure difference over the valve as well as changes in density (volume expansion $\hat{V}_\mathrm{e}/\hat{V}_\mathrm{i} = \rho_\mathrm{i}/\rho_\mathrm{e}$), and the valve opening A_e vs. full opening A_i.

In reality, adaptations of Bernoulli's law are used, as in the sequel.

ISA incompressible fluid Instrument Society of America defines valve models in the ANSI/ISA S75.01 standard[9] for *incompressible* (i.e., $\dot{V}_\mathrm{i} = \dot{V}_\mathrm{e} = \dot{V}$), non-choked fluids without fitting as

$$C = \frac{\dot{V}}{N_1}\sqrt{\frac{\rho_\mathrm{i}/\rho^\varsigma}{p_\mathrm{i} - p_\mathrm{e}}}. \tag{20}$$

Here, C is the valve coefficient, while ρ^ς is a scaling density such that $\rho_\mathrm{i}/\rho^\varsigma$ represents specific gravity. For liquids, water at 1 atm and 15.56 °C (60 F) is often used as scaling density in specific gravity, with $\rho^\varsigma \approx 1000\,\mathrm{kg/m^3}$ in SI units. The value of C is found as the flow rate through the valve for a reference fluid (water for liquids, i.e., $\rho_\mathrm{i}/\rho^\varsigma \equiv 1$) with a *unit* pressure drop $p_\mathrm{i} - p_\mathrm{e}$, while N_1 handles unit conversion.

Specifically, the expression in Eq. 20 has the following meaning:

1. With pressure in units psi (pressure per square inch) and volumetric flow rate $\dot{V}$ in gal/min (gallons per minute), valve coefficient C is named the *flow coefficient* denoted by C_v, and $N_1 \equiv 1$. Using water as fluid with pressure difference $p_\mathrm{i} - p_\mathrm{e} = 1\,\mathrm{psi}$, C_v equals the observed flow rate $\dot{V}$.

2. With arbitrary liquids, the flow rate is then given (in gal/min) by

$$\dot{V} = C_\mathrm{v}N_1\sqrt{\frac{p_\mathrm{i} - p_\mathrm{e}}{\rho_\mathrm{i}/\rho^\varsigma}}$$

   when pressure is given in psi and $N_1 = 1$.

3. If we choose other units, N_1 is changed to handle the unit conversion. As an example, if pressure is given in unit bar and the flow rate $\dot{V}$ is desired in $\mathrm{m^3/h}$, we need to use $N_1 = 8.65 \cdot 10^{-1}$.

4. For other units, other values of N_1 must be used. Thus, when we use symbol C_v, the natural units (i.e., $N_1 = 1$) are pressure in psi and flow rate in gal/min.

[9] `http://integrated.cc/cse/ISA_750101_SPBd.pdf`

5. If we instead want to use as natural units pressure in bar and flow rate in m^3/h (metric units), we use symbol K_v for valve coefficient and name it the *flow factor*. In that case,
$$\dot{V} = K_v N_1 \sqrt{\frac{p_i - p_e}{\rho_i/\rho^\varsigma}}.$$
With pressure p in unit bar and flow rate in m^3/h, $N_1 = 1$.

6. If we know K_v and instead want to use pressure units kPa and flow rate m^3/h, we need to set $N_1 = 0.1$. Etc.

Control valves When we have control valves, C_v and K_v become functions of the control signal/valve opening u_v, $C_v(u_v)$ and $K_v(u_v)$.

ISA incompressible fluid: dimensionless form Instead of adjusting N_1 to handle different unit choices, it would be better to pose the valve model in dimensionless form as
$$\frac{\dot{V}}{C_{\dot{V}}} = \sqrt{\frac{(p_i - p_e)/p^\varsigma}{\rho_i/\rho^\varsigma}}. \tag{21}$$
Here, $C_{\dot{V}}$ plays the role of $C_v N_1/\sqrt{p^\varsigma}$ or $K_v N_1/\sqrt{p^\varsigma}$.

For the dimensionless description in Eq. 21, we will express a variable valve opening as $C_{\dot{V}} \cdot f(u_v)$ where $u_v \in [0,1]$ and $f : [0,1] \to [0,1]$ is the valve characteristic, i.e., we will modify Eq. 21 into
$$\dot{V} = C_{\dot{V}} \cdot f(u_v) \sqrt{\frac{(p_i - p_e)/p^\varsigma}{\rho_i/\rho^\varsigma}} \tag{22}$$
where now $C_{\dot{V}} \cdot f(u_v)$ plays the role of $C_v(u_v) N_1/\sqrt{p^\varsigma}$ or $K_v(u_v) N_1/\sqrt{p^\varsigma}$.

ISA compressible fluid For *compressible*, non-choked fluids without fitting, ANSI/ISA S75.01 proposes the valve coefficient
$$C = \frac{\dot{m}}{N_6 \frac{\rho_i}{\rho_e} \sqrt{\frac{p_i - p_e}{\rho_i}}}$$
where the flow coefficient is named flow coefficient C_v when pressure is given in units psi, density is given in unit lb/ft^3, and mass flow is given in lb/h ("British" units). With these "standard" units, N_6 is given as $N_6 = 63.3$.

When metric units are used (pressure in bar, density in kg/m^3, flow rate in kg/h), the flow coefficient C is named the flow factor K_v, with $N_6 = 27.3$.

ISA compressible fluid: dimenionless form A dimensionless form of the valve model for compressible fluids is
$$\frac{\dot{m}}{C_{\dot{m}}} = \frac{\rho_i}{\rho_e} \sqrt{\frac{(p_i - p_e)/p^\varsigma}{\rho_i/\rho^\varsigma}} \tag{23}$$
where we for simplicity will choose $p^\varsigma = 1\,\text{bar} \approx 1\,\text{atm}$ (in the chosen unit) while $\rho^\varsigma = 1000\,kg/m^3$ and $\dot{m}$ will be given in unit kg/s. The valve coefficient will then also be given

in units kg/s, and it is trivial to convert $p^{\varsigma} = 1\,\text{bar}$, $\rho^{\varsigma} = 1000\,\text{kg/m}^3$, and $C_{\dot{m}}$ in kg/s to other units.

For the case of a control valve, we will describe the flow of compressible fluids as

$$\dot{m} = C_{\dot{m}} \cdot f\left(u_{\text{v}}\right) \frac{\rho_{\text{i}}}{\rho_{\text{e}}} \sqrt{\frac{\left(p_{\text{i}} - p_{\text{e}}\right)/p^{\varsigma}}{\rho_{\text{i}}/\rho^{\varsigma}}} \tag{24}$$

where $u_{\text{v}} \in [0, 1]$ is the valve control signal, and $f : [0, 1] \to [0, 1]$ is the valve characteristics.

One-directional valve Note that in the above expressions, the choice of influent and effluent pressures, p_{i} and p_{e}, is so that the highest pressure is deemed the influent pressure. In case of change of which pressure is highest, this will lead to flow reversal, and extreme care must be shown. If the valve is a one-way valve, i.e., fluid can only flow in one direction, this can be fixed by changing

$$p_{\text{i}} - p_{\text{e}} \to \max\left(p_{\text{i}} - p_{\text{e}}, 0\right).$$

2.4.4 Pipe friction

The friction drop along the pipe can be given by the Darcy-Weisbach model (Lie 2022) as

$$\frac{\Delta p_{\text{f}}}{\ell} = f_{\text{D}} \frac{\rho}{2} \frac{v^2}{D} \tag{25}$$

where f_{D} is Darcy's friction factor, given by Colebrook's[10] implicit expression

$$\frac{1}{\sqrt{f_{\text{D}}}} = -2 \cdot \log_{10}\left(\frac{2.51}{N_{\text{Re}}} \cdot \frac{1}{\sqrt{f_{\text{D}}}} + \frac{\epsilon/D}{3.71}\right) \tag{26}$$

where $N_{\text{Re}} = \frac{\rho v D}{\mu} = \frac{vD}{\nu}$ is the Reynolds number, μ is *dynamic* viscosity, ν is *kinematic* viscosity (v is velocity), and ϵ is the "roughness height" of the pipe internals.

A number of explicit approximations for f_{D} in the Colebrook equation exists, see lecture notes. A simple approximation could be the Swamee and Jain approximation, Lie (2022),

$$\frac{1}{\sqrt{f_{\text{D}}}} = -2 \cdot \log_{10}\left(\frac{5.74}{N_{\text{Re}}^{0.9}} + \frac{\epsilon/D}{3.7}\right). \tag{27}$$

3 Project tasks

3.1 Generic models

Density

We consider an oil-water mixture without gas, thus a pure liquid. Let ρ_{o} be the crude oil density and ρ_{w} the water density. We denote the *water cut* by χ_{w},

$$\chi_{\text{w}} \triangleq \frac{\dot{V}_{\text{w}}}{\dot{V}} \Rightarrow \dot{V}_{\text{w}} = \chi_{\text{w}} \dot{V} \tag{28}$$

[10] The Colebrook equation, or sometimes known as the Colebrook-White equation.

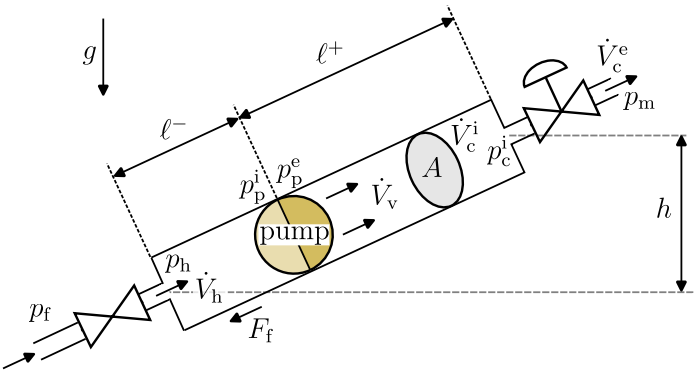

Figure 17: System from reservoir formation to manifold. Although the pipe string is vertical as in Fig. 7, for generality the pipe is depicted as sloping in this figure.

where $\dot{V}_w$ is the volumetric flow rate of water, while $\dot{V}$ is the total volumetric flow rate. We will also assume an *ideal solution*, which implies that

$$\dot{V} = \dot{V}_w + \dot{V}_o. \tag{29}$$

Problem 1. Total density of liquid mixture

Defining total/mixture density ρ as $\rho \triangleq \dot{m}/\dot{V}$ where $\dot{m}$ is total mass flow, *show* that we can express ρ as

$$\rho = \chi_w \rho_w + (1 - \chi_w)\, \rho_o. \tag{30}$$

▲

Problem 2. EoS for liquid mixture

With reference to Section 2.3.1:

1. Show that if we neglect the temperature dependence of ρ, $\mathrm{d}\rho$ can be expressed as

$$\mathrm{d}\rho \approx \rho \beta_T \mathrm{d}p. \tag{31}$$

2. Show that if we furthermore assume that β_T is constant and independent of pressure, we can express the density as

$$\rho = \rho_0 \exp\left(\beta_T \left(p - p_0\right)\right), \tag{32}$$

where the density is ρ_0 at some reference pressure p_0. ▲

Observe that the *isothermal compressibility* β_T from thermodynamics used here, is the *inverse* of the so-called *bulk modulus* β from mechanical engineering.

3.2 Single well from reservoir formation to manifold

We consider first the pipe string system in Fig. 17.

In this system, we will assume that reservoir formation pressure p_f, the manifold pressure p_m, the rotational (electrical submersed) pump frequency/speed f_p, and choke

valve signal u_v are input variables and known functions of time, i.e., the vector of inputs u is

$$u = (p_\mathrm{f}, p_\mathrm{m}, f_\mathrm{p}, u_\mathrm{v})\,. \tag{33}$$

We will be interested in finding the response in flow rate and pressure drop through the system.

Based on the indicated variation in liquid density in Fig. 10, we will *for simplicity* assume that the fluid density is constant from reservoir to manifold.

Problem 3. Pressure variation in pipe string

We will assume that the fluid density in the pipe string system is approximately constant.

- With the density as a function of pressure, $\rho\,(p)$, as in Eq. 32, does this mean that we can assume that the pressure is constant throughout the pipe string? ▲

Problem 4. Mass balance

1. In Fig. 17, we can identify three pieces of "equipment": (i) the "valve" from formation pressure p_f to heel pressure p_h, Eq. 16, the pump (ESP) from pressure p_p^i to p_p^e, Eqs. 17–18, and the choke valve from pressure p_c^i to manifold pressure p_m, Eq. 24.

   Will liquid mass be *accumulated* ($\mathrm{d}m/\mathrm{d}t \neq 0$) in these pieces of equipment, or can we assume that there is no mass accumulated in them ($\mathrm{d}m/\mathrm{d}t = 0$)?

2. With the assumption of constant density in the pipe itself, is it possible that there is mass accumulation in the pipe?

3. What are the consequences of your findings in points 1–2 above wrt. flow rate $\dot{V}_\mathrm{v}$ in the vertical pipe? ▲

◊ ◊ ◊

The general momentum balance can be written as

$$\frac{\mathrm{d}\mathfrak{m}}{\mathrm{d}t} = \dot{\mathfrak{m}}_\mathrm{i} - \dot{\mathfrak{m}}_\mathrm{e} + F \tag{34}$$

where momentum $\mathfrak{m}$ and momentum flow $\dot{\mathfrak{m}}$ in the one-dimensional direction can be expressed as

$$\mathfrak{m} \triangleq mv \tag{35}$$

$$\dot{\mathfrak{m}} \triangleq \dot{m}v \tag{36}$$

and v is linear velocity.

The involved forces in F are related to:

- Pressure forces at inlet and outlet of the pipe,

$$F_p = p_\mathrm{h}A - p_\mathrm{c}^\mathrm{i}A \tag{37}$$

- Possible pressure boost due to a pump,

$$F_\mathrm{b} = \Delta p_\mathrm{p} A \tag{38}$$

- Friction loss,
$$F_{\mathrm{f}} = \Delta p_{\mathrm{f}} A \tag{39}$$
- Flow against gravity, with a lifth height h,
$$F_{\mathrm{g}} = \Delta p_{\mathrm{g}} A, \tag{40}$$
with
$$\Delta p_{\mathrm{g}} = \rho_{\mathrm{v}} g h.$$

Consider the pipe string from the heel to the inlet of the choke valve.

Problem 5. Total force F in momentum balance

1. Express the total force F consisting of forces F_{p} (inlet, outlet pressure), F_{b} ("booster" pump), F_{f} (friction), F_{g} (gravity) [**hint:** including signs].
2. Identify which model given in this document is relevant for the pressure changes Δp_{p} and Δp_{f}.

▲

Problem 6. Flow equation from momentum balance

1. Assuming ideal mixing, show that the linear velocity v_{v} through the vertical pipe is given by
$$m_{\mathrm{v}} \frac{\mathrm{d}v_{\mathrm{v}}}{\mathrm{d}t} = F. \tag{41}$$
2. Show that the volumetric flow rate $\dot{V}_{\mathrm{v}}$ through the pipe can be developed from Eq. 41 and your expression for the total force to become
$$\frac{\mathrm{d}\dot{V}_{\mathrm{v}}}{\mathrm{d}t} = \frac{A_{\mathrm{v}}}{\rho_{\mathrm{v}} \ell} \left(p_{\mathrm{h}} - p_{\mathrm{c}}^{\mathrm{i}} + \Delta p_{\mathrm{p}} - \Delta p_{\mathrm{f}} - \Delta p_{\mathrm{g}} \right). \tag{42}$$

▲

Problem 7. Complete model from reservoir formation to manifold

In addition to the model in Eq. 42, you need expressions for Δp_{p}, Δp_{f}, and Δp_{g}. Furthermore, you need expressions for $\dot{V}_{\mathrm{h}}$ and for flow through the choke valve.

1. List the concrete expressions for Δp_{p}, Δp_{f}, and Δp_{g}, as well as for $\dot{V}_{\mathrm{h}}$ and the flow through the choke valve.

   Add any possible additional equations that you need.
2. Explain how you in Eq. 42 can express $p_{\mathrm{h}} = p_{\mathrm{h}}\left(\dot{V}_{\mathrm{v}}, p_{\mathrm{f}}\right)$, $\Delta p_{\mathrm{p}} = \Delta p_{\mathrm{p}}\left(\dot{V}_{\mathrm{v}}, f_{\mathrm{p}}\right)$, $\Delta p_{\mathrm{f}} = \Delta p_{\mathrm{f}}\left(\dot{V}_{\mathrm{v}}\right)$, Δp_{g}, and $p_{\mathrm{c}}^{\mathrm{i}} = p_{\mathrm{c}}^{\mathrm{i}}\left(\dot{V}_{\mathrm{v}}, p_{\mathrm{m}}, u_{\mathrm{v}}\right)$.

   Explain why the expressions for p_{h}, Δp_{p}, Δp_{f}, Δp_{g}, and $p_{\mathrm{c}}^{\mathrm{i}}$ are important for

   (a) Posing the model in State Space form

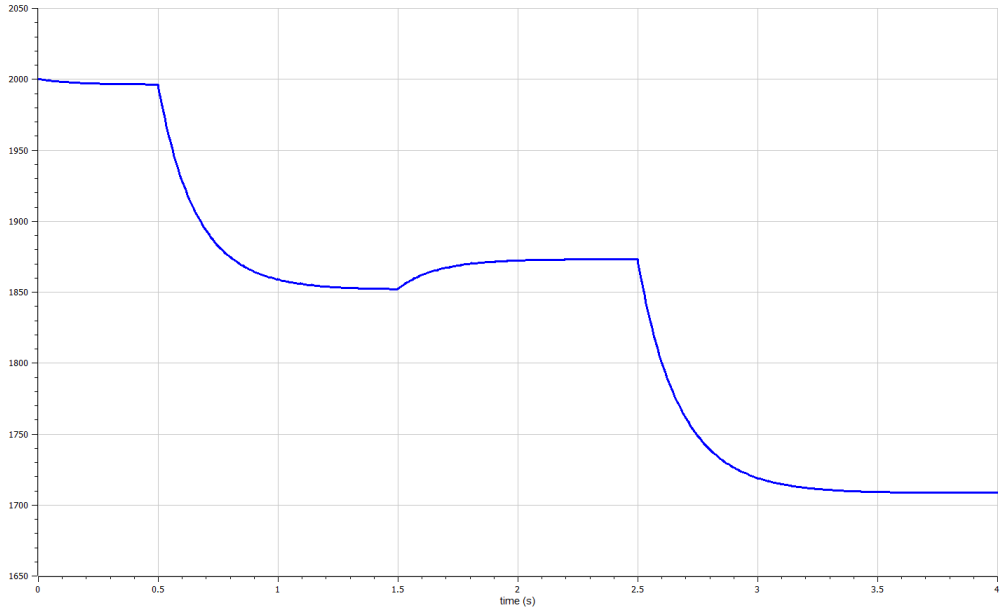

Figure 18: Indication of vertical volumetric flow rate $\dot{V}_\mathrm{v}$ (unit: m^3/d) with data from Appendix A.

(b) Implementing the model in languages with ODE solvers without access to DAE solvers.

▲

◊ ◊ ◊

In course FM1015, the favored model formulation is Differential Algebraic Equations (DAE), where DAE solvers are needed to find the solution (e.g., OpenModelica and Julia have good DAE solvers). The most elegant way to do this is to pose the momentum balance directly, in this case as

$$\frac{\mathrm{d}\mathfrak{m}}{\mathrm{d}t} = F$$

and then add algebraic equations to define $\mathfrak{m}$ and F. However, the resulting DAE may become difficult to solve (e.g., for the OpenModelica solver), and in this case, it is recommended to instead use the model in Eq. 42 — which is derived from the above momentum balance. You can then choose whether you pose the model as an ODE or a DAE.

3.3 Simulation of single well from formation to manifold

Problem 8. Single well model from reservoir formation to manifold

1. Implement the model of the single well from formation to manifold in your chosen language. Use the model parameters and operating conditions given in Appendix A, and simulate the system.

2. Verify that your vertical pipe flow rate $\dot{V}_\mathrm{v}$ responds similarly to in Fig 18. and that the pressure p_c^i in front of the choke valve responds similarly to in Fig. 19.

▲

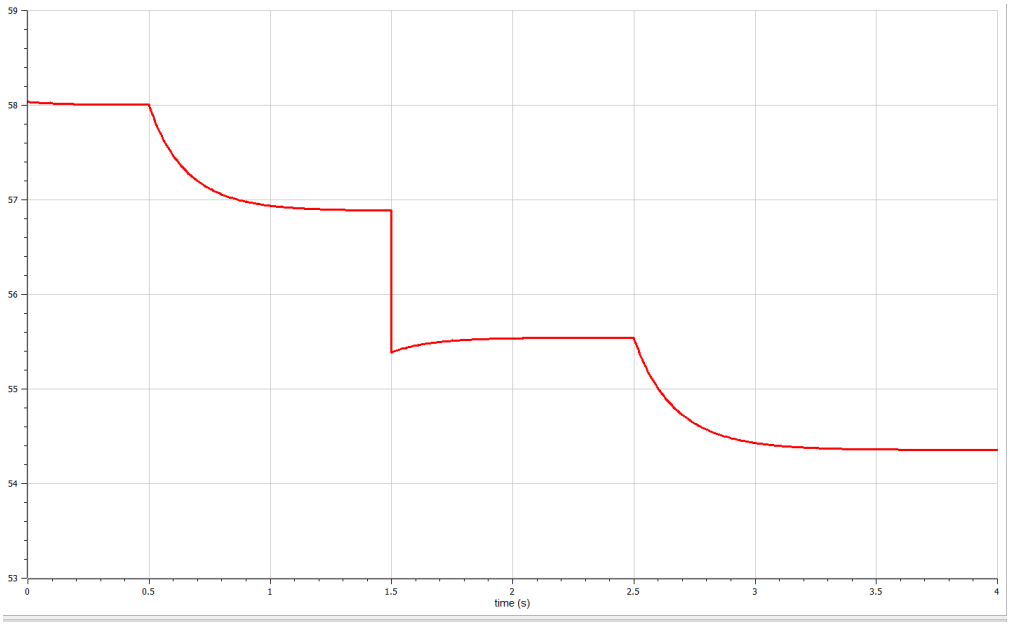

Figure 19: Indication of pressure $p_{\mathrm{c}}^{\mathrm{i}}$ (unit: bar) with data from Appendix A.

3.4 Manifold model

To reduce fluid friction in the pipe from the manifold to the separator, we seek to reduce the viscosity of the fluid in the manifold from water cut χ_{w} in the production fluid to a water cut $\chi_{\mathrm{w}}^{\mathrm{m}}$ for the manifold by adding pure water into the manifold at flow rate $\dot{V}_{\mathrm{w}}$, see Fig. 7.

Assume that the manifold volume in Fig. 7 is well stirred, with a single influent volumetric flow rate $\dot{V}_{\mathrm{c}}^{\mathrm{e}}$ from a vertical pipe, a single influent pure water volumetric flow rate $\dot{V}_{\mathrm{w}}$, and a single effluent volumetric flow rate $\dot{V}_{\mathrm{s}}$ towards the separator. Assume furthermore that the water cut in the manifold is at the desired value $\chi_{\mathrm{w}}^{\mathrm{m}}$.

Problem 9. Ideal water flow rate for single well case

1. Show that by choosing $\dot{V}_{\mathrm{w}}$ as

$$\dot{V}_{\mathrm{w}} = \frac{\chi_{\mathrm{w}}^{\mathrm{m}} - \chi_{\mathrm{w}}}{1 - \chi_{\mathrm{w}}^{\mathrm{m}}} \dot{V}_{\mathrm{c}}^{\mathrm{i}}, \tag{43}$$

   we will maintain a water cut $\chi_{\mathrm{w}}^{\mathrm{m}}$ in the manifold.

2. In practice, we can not achieve the ideal influent water flow rate $\dot{V}_{\mathrm{w}}$ in Eq. 43.
   (a) Why can we not achieve $\dot{V}_{\mathrm{w}}$ in Eq. 43 in practice?
   (b) How do we need to handle the problem of achieving $\chi_{\mathrm{w}}^{\mathrm{m}}$ in practice? ▲

In the sequel, we will, for simplicity, assume that we can compute $\dot{V}_{\mathrm{w}}$ as in Eq. 43.

Problem 10. Manifold pressure model for single well/single transport pipe case

1. Show that mass balance for the manifold leads to the differential equation

$$\frac{\mathrm{d}p_{\mathrm{m}}}{\mathrm{d}t} = \frac{1}{\rho_{\mathrm{m}} V_{\mathrm{m}} \beta_T} \left(\rho_{\mathrm{v}} \dot{V}_{\mathrm{v}} + \rho_{\mathrm{w}} \dot{V}_{\mathrm{w}} - \rho_{\mathrm{m}} \dot{V}_{\mathrm{s}} \right) \tag{44}$$

   where V_{m} is the manifold volume.

2. How would you compute ρ_{m} in Eq. 44? ▲

Next, we want to extend the model of the manifold to influents from n_{w} wells in addition to one influent of water, and n_{t} effluents to the separator.

Problem 11. Manifold pressure model for multiple well/multiple transport pipe case

1. Extend the expression for $\dot{V}_{\mathrm{w}}$ from the single well case of Eq. 43 to the multiple well case as in Fig. 9.

2. Extend the mass balance for the manifold with resulting manifold pressure equation from the single well case of Eq. 44 to the multiple well and multiple separator transport pipe case of Fig. 9. ▲

3.5 Multiple well model from formations to separator

We are now ready to formulate a complete model from several wells/formation pressures via the manifold and through multiple pipelines from the manifold to the separator.

Problem 12. Multiple well model

1. Explain how you can generalize the single well model from formation pressure to manifold in Section 3.2, and give equations from multiple wells/formation pressures to a common manifold.

2. Explain how the equations from multiple wells fits into the model of the manifold pressure for multiple well/multiple transport pipe case.

3. Show how you can modify the model of single well from formation pressure to manifold in Section 3.2 so that you instead describe a model from manifold pressure to separator pressure.

   (a) For simplicity, assume that the transport pipes from manifold to separator are horizontal.

   (b) For simplicity, replace the electric submersible pump with a "booster pump" which gives constant pressure increase Δp_{bp}.

   (c) For simplicity, assume that there is no pressure drop at the inlet valve to the separator, and that the pressure p_{s}^{-} at the end of the transport pipe equals the separator pressure p_{s}, Fig. 8. Assume that all transport pipes end up in the same separator. ▲

3.6 Simulation of multiple wells from formations to separator

Here, we will consider a case with $n_{\mathrm{w}} = 2$ (two wells) and $n_{\mathrm{t}} = 1$ (a single transport pipe from manifold to separator).

Problem 13. Two-well model from reservoir formation via manifold to separator

1. Implement the model of the system consisting of multiple wells from formations ($n_{\mathrm{w}} = 2$) via manifold to separator ($n_{\mathrm{t}} = 1$) in your chosen language. Use model parameters, suggest time functions for inputs, and use initial states from Appendix B.

2. Experiment with choosing identical, but also different Productivity Index constants for the two wells, taken from the set $\left\{C_{\dot{V}}^{\mathrm{pi}}, 0.7C_{\dot{V}}^{\mathrm{pi}}, 1.15C_{\dot{V}}^{\mathrm{pi}}, 1.6C_{\dot{V}}^{\mathrm{pi}}\right\}$ where $C_{\dot{V}}^{\mathrm{pi}}$ is the nominal value in Table 1. Check how this changes the solution of your model.

3. Choose at least one other model parameter or initial state, and simulate the system with some variation in this/these parameters to see how this changes the solution of your model. ▲

3.7 Documentation

Write a partial report and submit it in the Canvas group folder within the deadline. Write a technical report on the project and results (single file, maximum 15 pages + 1 cover page, PDF format) and submit the report in the Canvas group folder within the deadline. Prepare a "PowerPoint" presentation (= use PowerPoint or other tools) of 7 min for the oral presentation.

A Single well data

Parameters of a nominal vertical pipe are given in Table 1.

Initial state and nominal input values are given in Table 2.

B Multiple well data

Assume that both $n_{\mathrm{w}} = 2$ vertical pipes nominally have the same parameters, as in Table 1.

Parameters for the manifold and the single transport pipe ($n_{\mathrm{t}} = 1$) are given in Table 3.

Nominal values for initial states for the two vertical pipes can be chosen as in Table 2.

Nominal initial states and inputs for the manifold and the vertical transport pipe are as given in Table 4.

In Table 4, the nominal input functions of time are given as fixed values. You should suggest time functions similar to the time functions in Table 2.

References

Brauner, N. & Ullmann, A. (2002), 'Modeling of phase inversion phenomenon in two-phase pipe flows', *International Journal of Multiphase Flow* **28**, 1177–1204.

Bulgarelli, N. A. V., Buazussi, J. L., Monte Verde, W., Perles, C. E., de Castro, M. S. & Bannwart, A. C. (2021), 'Relative viscosity model for oil/water stable emulsion flow within electrical submersible pumps', *Chemical Engineering Science* **245**(116827).

Justiniano, M. & Romero, O. J. (2021), 'Inversion Point of Emulsions as a Mechanism of Head Loss Reduction in Onshore Pipeline Heavy Oil Flow', *Brazilian Journal of Petroleum and Gas* **15**(1–2), 13–24.

Lie, B. (2022), Modeling of dynamic systems. Lecture notes in course FM1015 at University of South-Eastern Norway.

Table 1: Parameters for the nominal vertical pipe.

Parameter	Value	Parameter
ℓ^-	$100\,\mathrm{m}$	Vertical pipe below pump
ℓ^+	$2000\,\mathrm{m}$	Vertical pipe above pump
d	$0.1569\,\mathrm{m}$	Vertical pipe diameter
β_T	$\frac{1}{1.5\cdot 10^9} \approx 6.67 \cdot 10^{-10}\,\mathrm{Pa}^{-1}$	Isothermal compressibility of fluid
p_0	$1\,\mathrm{bar}$	Pressure at which ρ_0 is known, Eq. 32.
ρ_o	$900\,\mathrm{kg/m^3}$	Crude oil density
ρ_w	$1000\,\mathrm{kg/m^3}$	Water density
χ_w	0.35	Inlet water cut
ρ_0	$\chi_\mathrm{w}\rho_\mathrm{w} + (1-\chi_\mathrm{w})\,\rho_\mathrm{o}$	Density of mixture at pressure p_0, Eq. 32.
ν_o	$100\,\mathrm{cSt} = 100 \cdot 10^{-6}\,\mathrm{m^2/s}$	Kinematic viscosity of oil
ν_w	$1\,\mathrm{cSt} = 10^{-6}\,\mathrm{m^2/s}$	Kinematic viscosity of water
ϵ	$0.0018\,\mathrm{inch} = 45.7\,\mu\mathrm{m} = 45.7 \cdot 10^{-6}\,\mathrm{m}$	Pipe roughness dimension
h_p^ς	$1210.6\,\mathrm{m}$	Pump scaling head
$f_{\mathrm{p},0}$	$60\,\mathrm{Hz}$	Nominal pump frequency
$\dot{V}^\varsigma$	$1\,\mathrm{m^3/s}$	Pump scaling flow rate, Eq. 18
a_1	-37.57	ESP parameters, Eq. 18
a_2	$2.864 \cdot 10^3$	— " —
a_3	$-8.668 \cdot 10^4$	— " —
$C_{\dot{m}}$	$25.9 \cdot 10^3\,\mathrm{kg/h}$	Valve capacity in Eq. 24, with $p^\varsigma = 1\,\mathrm{bar}$ and $\rho^\varsigma = 10^3\,\mathrm{kg/m^3}$
$f(u_\mathrm{v})$	$\begin{cases} 0, & u_\mathrm{v} \le 0.05 \\ \frac{11.1u_\mathrm{v}-0.556}{30}, & 0.05 < u_\mathrm{v} \le 0.5 \\ \frac{50u_\mathrm{v}-20}{30}, & 0.5 < u_\mathrm{v} \le 1 \end{cases}$	Choke valve characteristic, with $u_\mathrm{v} \in [0,1]$
$C_{\dot{V}}^\mathrm{pi}$	$7 \cdot 10^{-4}\,\mathrm{m^3/s}$	Productivity Index constant with $p_\mathrm{pi}^\varsigma = 1\,\mathrm{bar}$, Eq. 16

Table 2: Operating conditions for the nominal vertical pipe.

Variable	Value	Parameter
$p_\mathrm{c}^\mathrm{i}(t=0)$	$55\,\mathrm{bar} = 55 \cdot 10^5\,\mathrm{Pa}$	Initial pressure: *not a state*, but useful for helping solver
$\dot{V}_\mathrm{v}(t=0)$	$2000\,\mathrm{m^3/d} \approx 0.02315\,\mathrm{m^3/s}$	Initial volumetric flow rate
$p_\mathrm{f}(t)$	$\begin{cases} 220\,\mathrm{bar}, & t < 0.5\,\mathrm{s} \\ 0.95 \cdot 220\,\mathrm{bar}, & t \ge 0.5\,\mathrm{s} \end{cases}$	Reservoir formation pressure
$p_\mathrm{m}(t)$	$\begin{cases} 50\,\mathrm{bar}, & t < 1.5\,\mathrm{s} \\ 0.97 \cdot 50\,\mathrm{bar}, & t \ge 1.5\,\mathrm{s} \end{cases}$	Manifold pressure
$f_\mathrm{p}(t)$	$\begin{cases} 60\,\mathrm{Hz}, & t < 2.5\,\mathrm{s} \\ 0.95 \cdot 60\,\mathrm{Hz}, & t \ge 2.5\,\mathrm{s} \end{cases}$	Pump rotational frequency
$u_\mathrm{v}(t)$	1.0	Choke valve opening

Table 3: Nominal parameters for manifold and transport pipe.

Parameter	Value	Parameter
ℓ_{m}	$500\,\mathrm{m}$	Manifold length
d_{m}	$0.1569\,\mathrm{m}$	Manifold diameter
β_T	$\frac{1}{1.5\cdot 10^9} \approx 6.67 \cdot 10^{-10}\,\mathrm{Pa}^{-1}$	Isothermal compressibility of fluid
p_0	$1\,\mathrm{bar}$	Pressure at which ρ_0 is known, Eq. 32.
ρ_{o}	$900\,\mathrm{kg/m^3}$	Crude oil density
ρ_{w}	$1000\,\mathrm{kg/m^3}$	Water density
$\chi_{\mathrm{w}}^{\mathrm{m}}$	0.5	Manifold-to-separator water cut
ρ_0	$\chi_{\mathrm{w}}^{\mathrm{m}}\rho_{\mathrm{w}} + (1-\chi_{\mathrm{w}}^{\mathrm{m}})\,\rho_{\mathrm{o}}$	Density of mixture at pressure p_0, Eq. 32.
ν_{o}	$100\,\mathrm{cSt} = 100 \cdot 10^{-6}\,\mathrm{m^2/s}$	Kinematic viscosity of oil
ν_{w}	$1\,\mathrm{cSt} = 10^{-6}\,\mathrm{m^2/s}$	Kinematic viscosity of water
ℓ_{t}	$4000\,\mathrm{m}$	Length of horizontal transport pipe
d_{t}	$0.1569\,\mathrm{m}$	Diameter of horizontal transport pipe
ϵ	$0.0018\,\mathrm{inch} = 45.7\,\mu\mathrm{m} = 45.7 \cdot 10^{-6}\,\mathrm{m}$	Pipe roughness dimension
$\Delta p_{\mathrm{bp}}^{\mathrm{s}}$	$10\,\mathrm{bar}$	Booster pump scaling pressure increase
$f_{\mathrm{bp},0}$	$60\,\mathrm{Hz}$	Nominal buster pump frequency; $f_{\mathrm{bp},0} = f_{\mathrm{bp}}^{\max}$

Table 4: Nominal initial states for the manifold and horizontal transport pipe. Nominal inputs to the system.

Variable	Value	Parameter
$p_{\mathrm{m}}\,(t=0)$	$50\,\mathrm{bar} = 50 \cdot 10^5\,\mathrm{Pa}$	Initial manifold pressure
$\dot{V}_{\mathrm{t}}\,(t=0)$	$2000\,\mathrm{m^3/d} \approx 0.02315\,\mathrm{m^3/s}$	Initial volumetric flow rate
p_{f}	$220\,\mathrm{bar}$	Reservoir formation pressure
$p_{\mathrm{s}} = p_{\mathrm{s}}^{-}$	$30\,\mathrm{bar}$	Separator pressure
f_{p}	$60\,\mathrm{Hz}$	Pump rotational frequency
u_{v}	1.0	Choke valve opening
f_{bp}	$60\,\mathrm{Hz}$	Maximum frequency of booster pump

Sharma, R. (2014), Optimal Operation of Gas Lifted and ESP Lifted Oil Fields: An Approach Based on Modeling, Simulation, Optimization and Control, PhD thesis, University of South-Eastern Norway, Kjølnes Ring 56, N-3918 Porsgrunn, Norway.